

**Electronic Supplementary Information (ESI)**

**Syntheses, structures and properties of group 12 element (Zn, Cd, Hg) coordination polymers with a mixed-functional phosphonate-biphenyl-carboxylate linker**

Christian Heering,<sup>a</sup> Biju Francis,<sup>a,b</sup> Bahareh Nateghi,<sup>a</sup> Gamall Makhloufi,<sup>a</sup> Steffen Lüdeke,<sup>c</sup> Christoph Janiak<sup>a</sup> \*

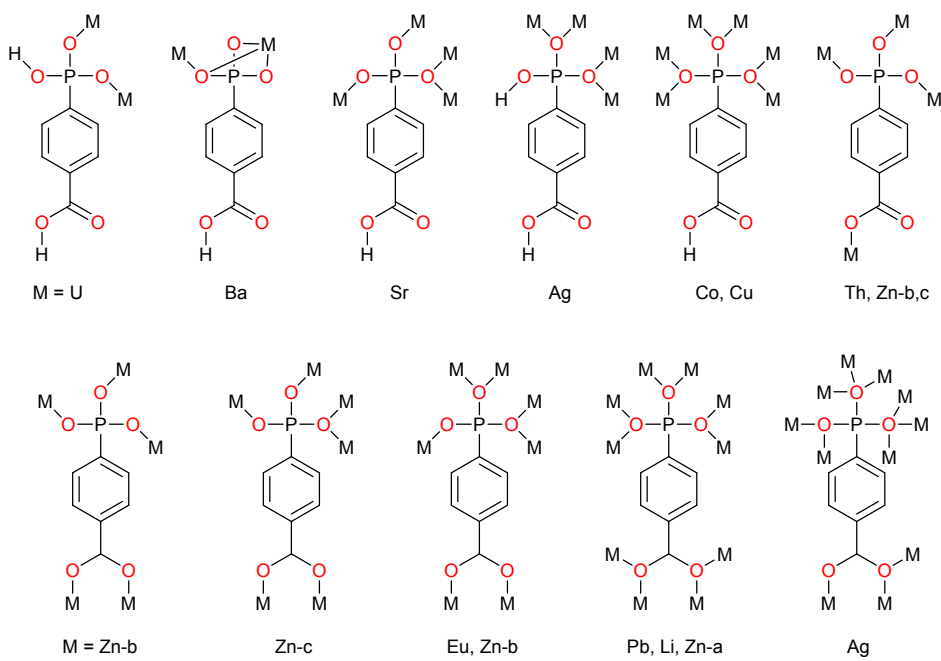
<sup>a</sup> Institut für Anorganische Chemie und Strukturchemie, Universität Düsseldorf, Universitätsstr. 1  
40225 Düsseldorf, Germany

<sup>b</sup> Permanent address: CSIR-Network of Institutes for Solar Energy  
National Institute for Interdisciplinary Science & Technology(NIIST) Thiruvananthapuram-695 019,  
India

<sup>c</sup> Institut für Pharmazeutische Wissenschaften, Universität Freiburg, Albertstr. 25  
79104 Freiburg

Emails: [christian.heering@hhu.de](mailto:christian.heering@hhu.de), [bijufrancis85@gmail.com](mailto:bijufrancis85@gmail.com), [Bahareh.Nateghi@hhu.de](mailto:Bahareh.Nateghi@hhu.de),  
[gamall.makhloufi@hhu.de](mailto:gamall.makhloufi@hhu.de), [steffen.luedeke@pharmazie.uni-freiburg.de](mailto:steffen.luedeke@pharmazie.uni-freiburg.de), [janiak@hhu.de](mailto:janiak@hhu.de)

<b>Content:</b>	<b>page</b>
<b>Coordination modes of the</b>	
<b>4-phosphonato-benzoic acid or -benzoate ligand</b>	<b>2</b>
<b>IR and NMR spectra</b>	<b>3-11</b>
<b>Thermogravimetric measurements</b>	<b>12-14</b>
<b>Powder X-ray diffraction patterns</b>	<b>15-16</b>
<b>Additional structure graphics</b>	<b>17-20</b>
<b>Structure tables</b>	<b>21-26</b>
<b>Supramolecular packing analyses</b>	<b>27-29</b>
<b>Cadmium distortion analysis</b>	<b>30</b>
<b>Circular dichroism spectra</b>	<b>31</b>



**Scheme S1** Coordination modes of the 4-phosphonato-benzoic acid or -benzoate ligand with different metal ions as published in literature. References are as follows:  
 barium,<sup>1</sup> cobalt,<sup>2</sup> copper,<sup>2</sup> europium,<sup>3</sup> lead,<sup>4</sup> lithium,<sup>5</sup> silver,<sup>6</sup> strontium,<sup>7</sup> thorium,<sup>8</sup> titanium,<sup>9</sup> uranium<sup>8</sup> and zinc-a<sup>5</sup>, -b<sup>10</sup>, -c.<sup>11</sup>

- 
- 1 J. Svoboda, V. Zima, L. Beneš, K. Melánová, M. Trchová and M. Vlček, *Solid State Sci.*, 2008, **10**, 1533-1542.
  - 2 A.-M. Pütz, L. M. Carrella and E. Rentschler, *Dalton Trans.*, 2013, **42**, 16194-16199.
  - 3 J.-M. Rueff, N. Barrier, S. Boudin, V. Dorcet, V. Caignaert, P. Boullay, G. B. Hix and P.-A. Jaffrès, *Dalton Trans.*, 2009, 10614–10620.
  - 4 J.-M. Rueff, O. Perez, A. Leclaire, H. Couthon-Gourvès and P.-A. Jaffrès, *Eur. J. Inorg. Chem.*, 2009, 4870–4876.
  - 5 J.-T. Li, L.-R. Guo, Y. Shen and L.-M. Zheng, *CrystEngComm*, 2009, **11**, 1674-1678.
  - 6 J.-M. Rueff, O. Perez, V. Caignaert, G. Hix, M. Berchel, F. Quentel and P.-A. Jaffrès, *Inorg. Chem.*, 2015, **54**, 2152–2159.
  - 7 V. Zima, J. Svoboda, L. Beneš, K. Melánová, M. Trchová and J. Dybal, *J. Solid State Chem.*, 2007, **180**, 929–939.
  - 8 P. O. Adelani and T. E. Albrecht-Schmitt, *Inorg. Chem.*, 2010, **49**, 5701–5705. P
  - 9 K. Melánová, J. Klevcov, L. Beneš, J. Svoboda and V. Zima, *J. Phys. Chem. Solids*, 2012, **73**, 1452–1455.
  - 10 J.-T. Li, D.-K. Cao, T. Akutagawa and L.-M. Zheng, *Dalton Trans.*, 2010, **39**, 8606-8608.
  - 11 Z. Chen, Y. Zhou, L. Weng and D. Zhao, *Cryst. Growth Des.*, 2008, **8**, 4045-4053.

## IR and NMR spectra

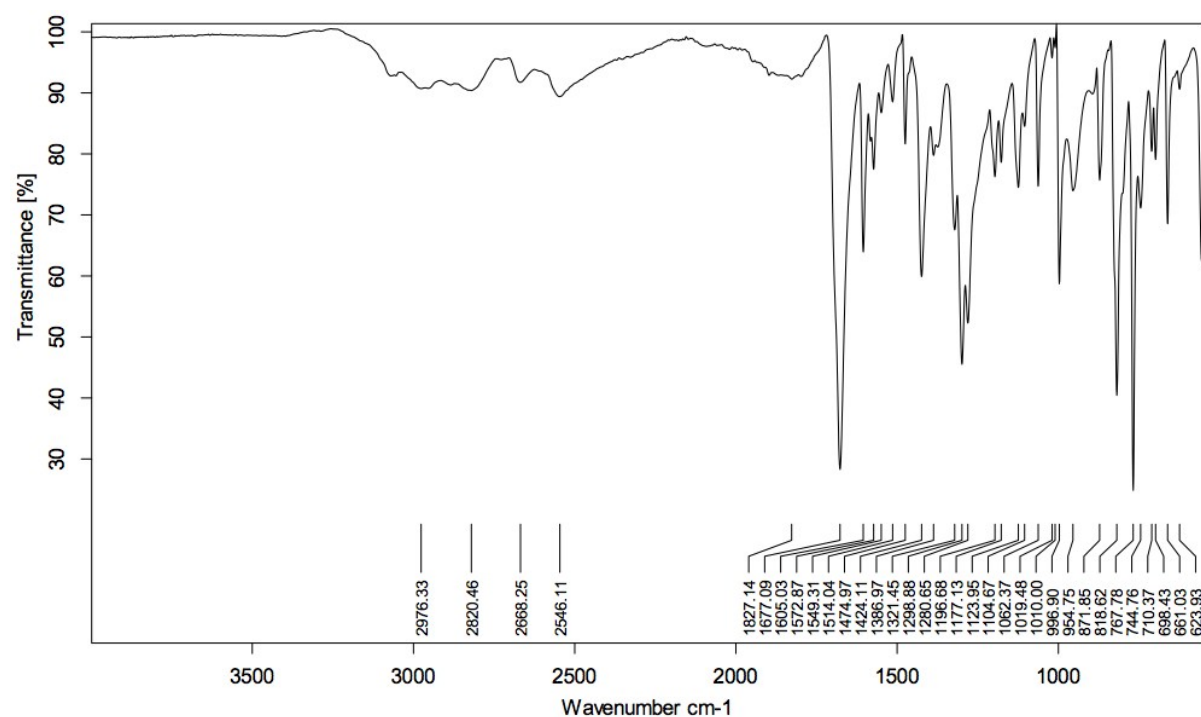


**Fig. S1** FT-IR (ATR) spectrum of 4-iodo-4'-biphenylcarboxylic acid, **1**.

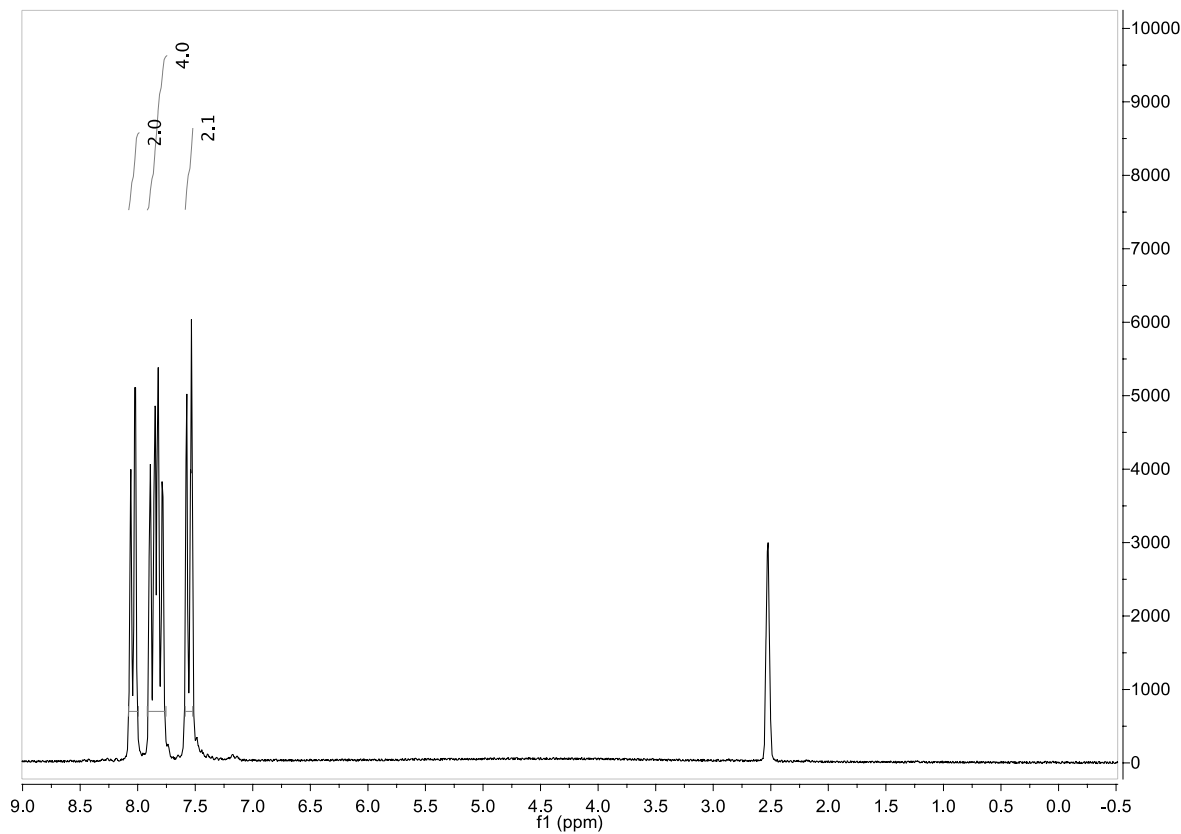


**Fig. S2**  $^1\text{H}$ -NMR spectrum of 4-iodo-4'-biphenylcarboxylic acid, **1** at 200 MHz in  $\text{DMSO}-d_6$ .

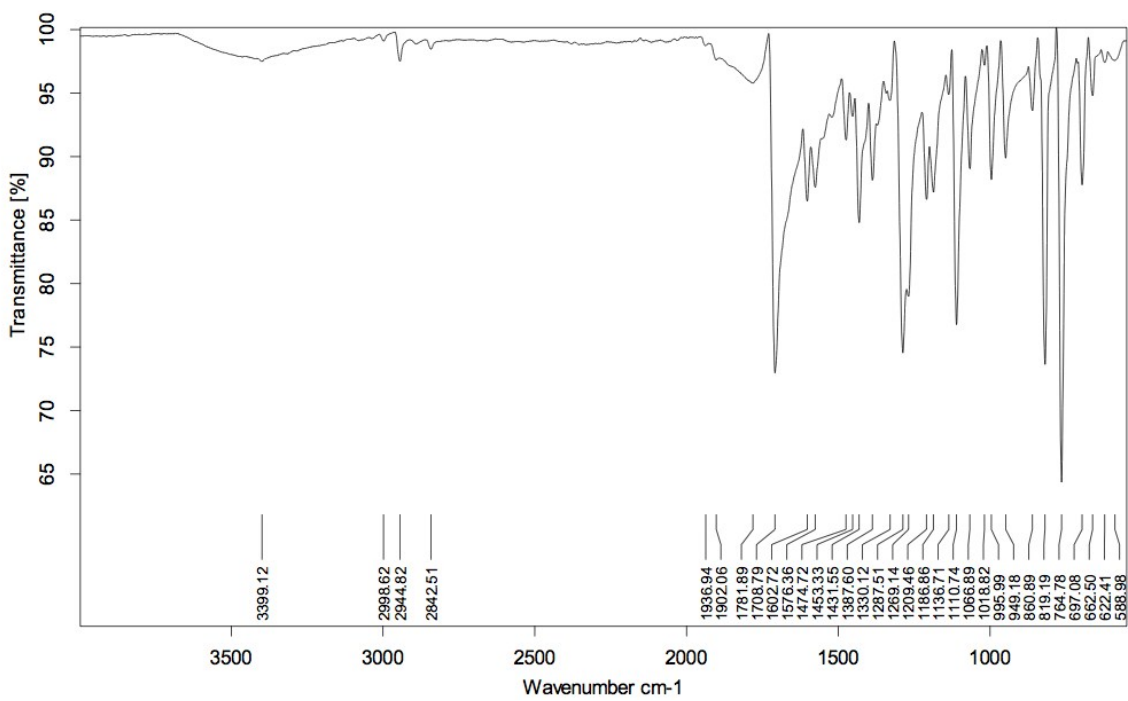


**Fig. S3** FT-IR (ATR) spectrum of 4-iodo-4'-biphenylcarboxylic acid methyl ester, **2**.

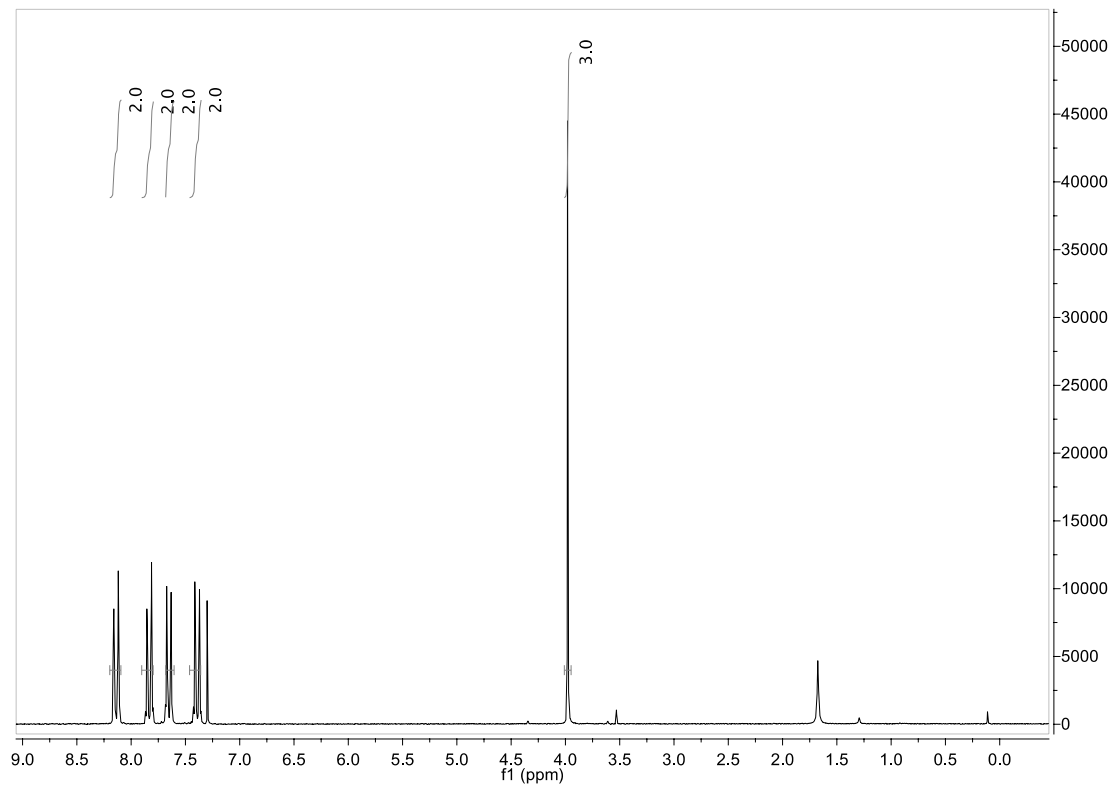


**Fig. S4**  $^1\text{H}$ -NMR spectrum of 4-iodo-4'-biphenylcarboxylic acid methyl ester, **2** at 200 MHz in  $\text{CDCl}_3$ .

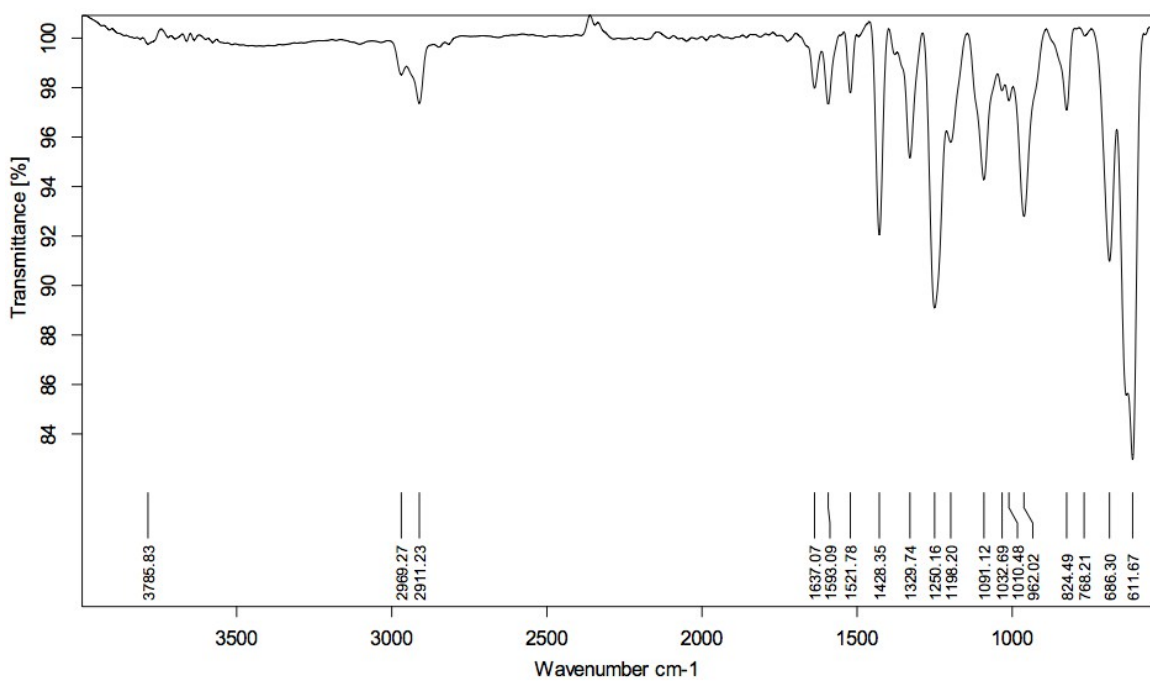


**Fig. S5** FT-IR (ATR) spectrum of 4-diethylphosphono-4'-biphenylcarboxylic acid methyl ester, **3**.

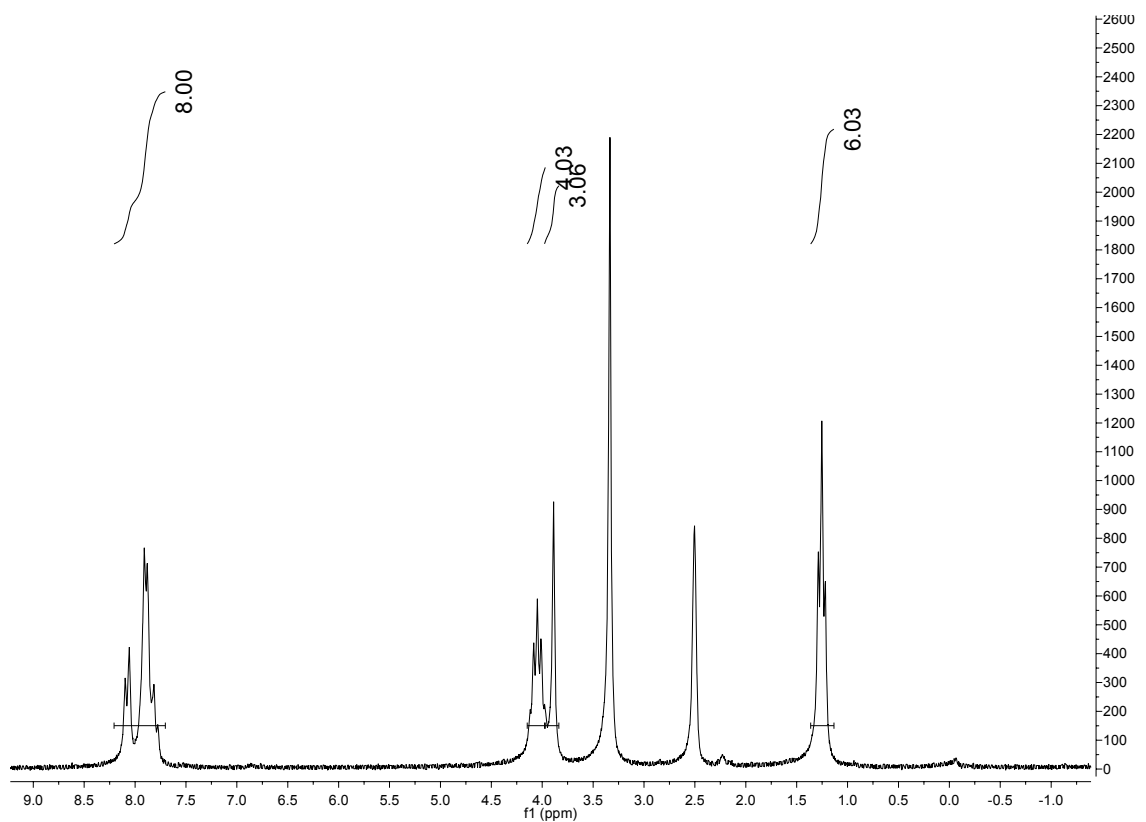


**Fig. S6**  $^1\text{H}$ -NMR spectrum of 4-diethylphosphono-4'-biphenylcarboxylic acid methyl ester, **3** at 200 MHz in  $\text{DMSO}-d_6$ .

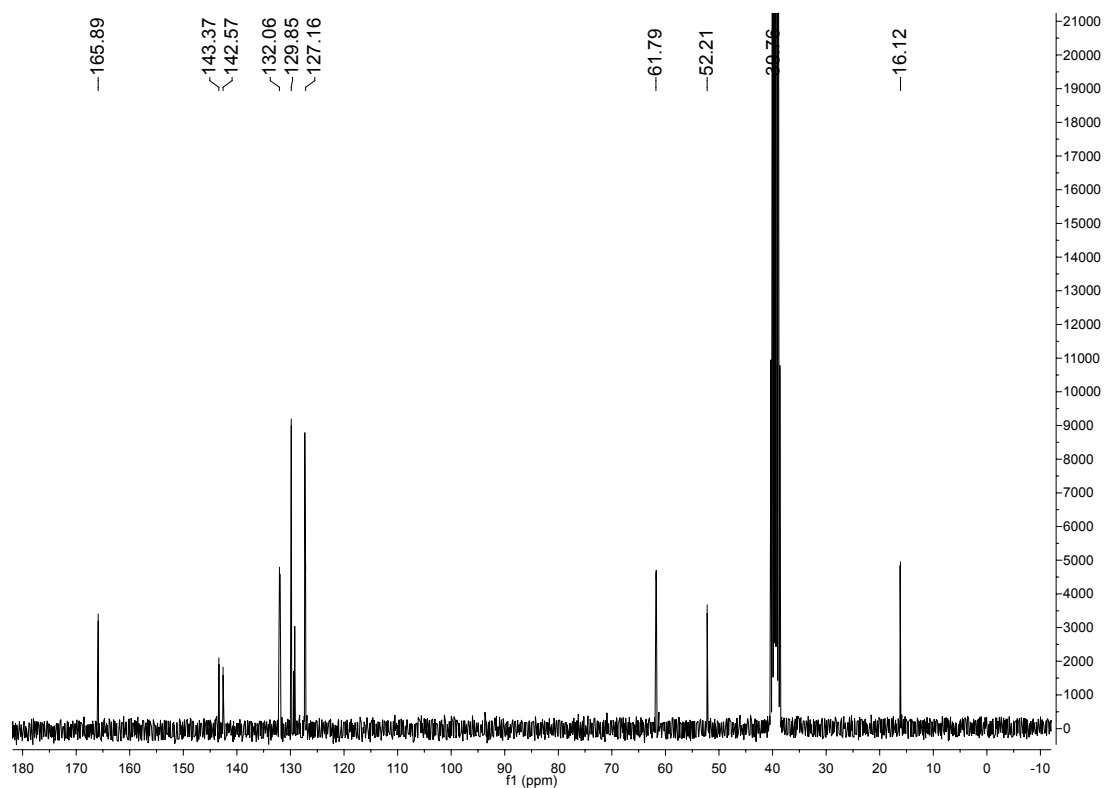


**Fig. S7**  $^{13}\text{C}$ -NMR spectrum of 4-diethylphosphono-4'-biphenylcarboxylic acid methyl ester, **3** at 75 MHz in  $\text{DMSO}-d_6$ .

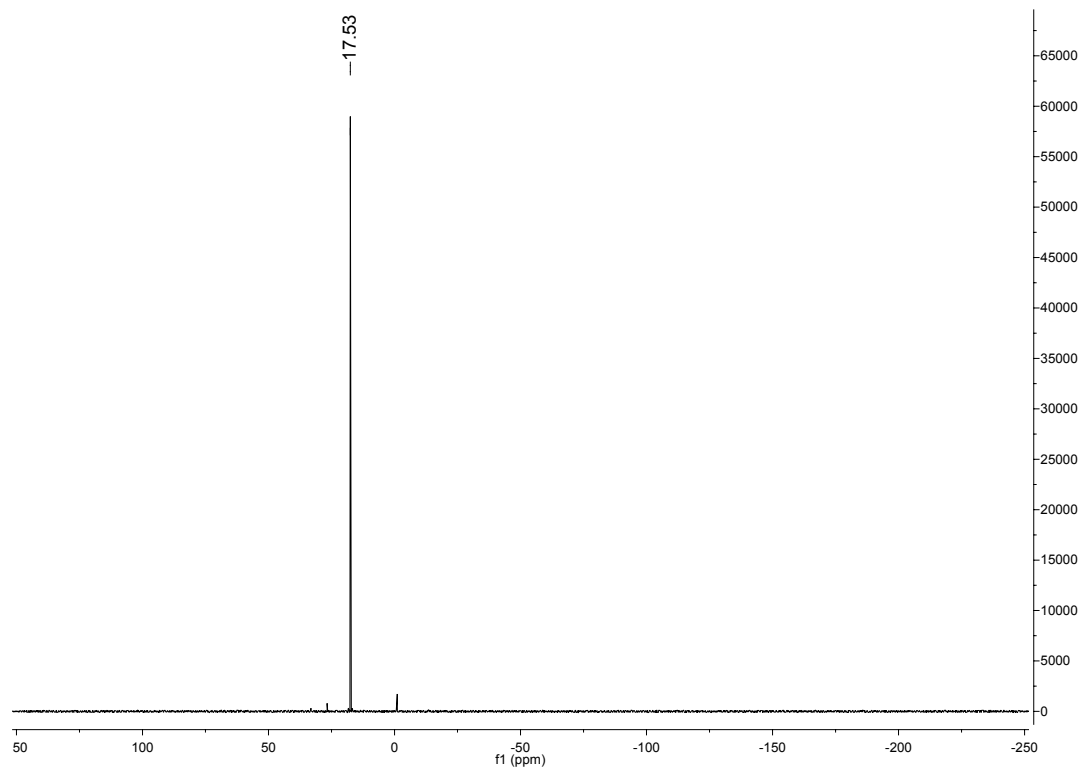


**Fig. S8**  $^{31}\text{P}\{\text{H}\}$ -NMR spectrum of 4-diethylphosphono-4'-biphenylcarboxylic acid methyl ester, **3** at 121 MHz in  $\text{DMSO}-d_6$ .

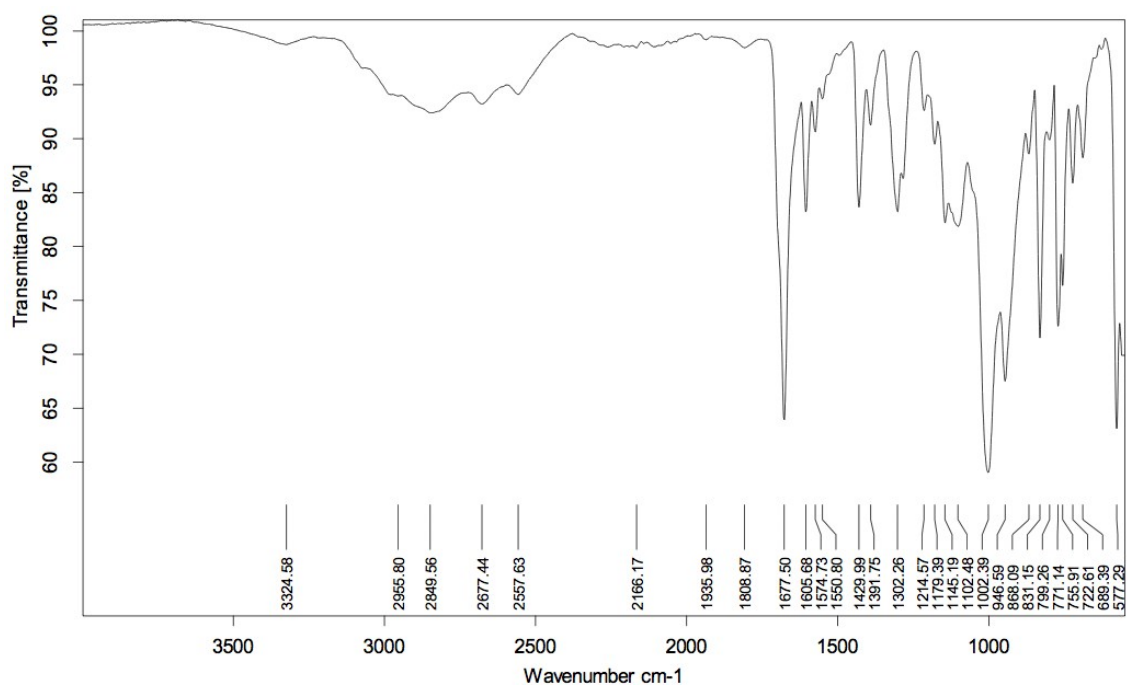


**Fig. S9** FT-IR (ATR) spectrum of 4-phosphonato-4'-biphenylcarboxylic acid, **4**.

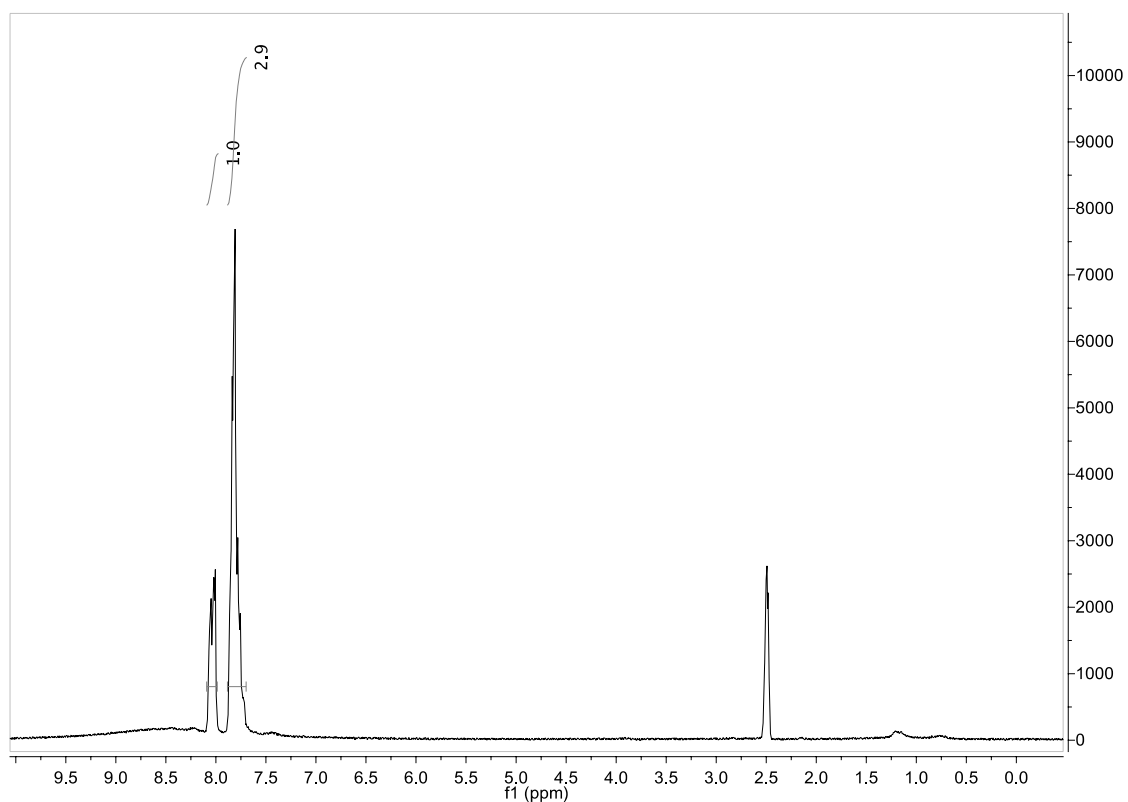


**Fig. S10**  $^1\text{H}$ -NMR spectrum of 4-phosphonato-4'-biphenylcarboxylic acid, **4** at 200 MHz in  $\text{DMSO}-d_6$ .

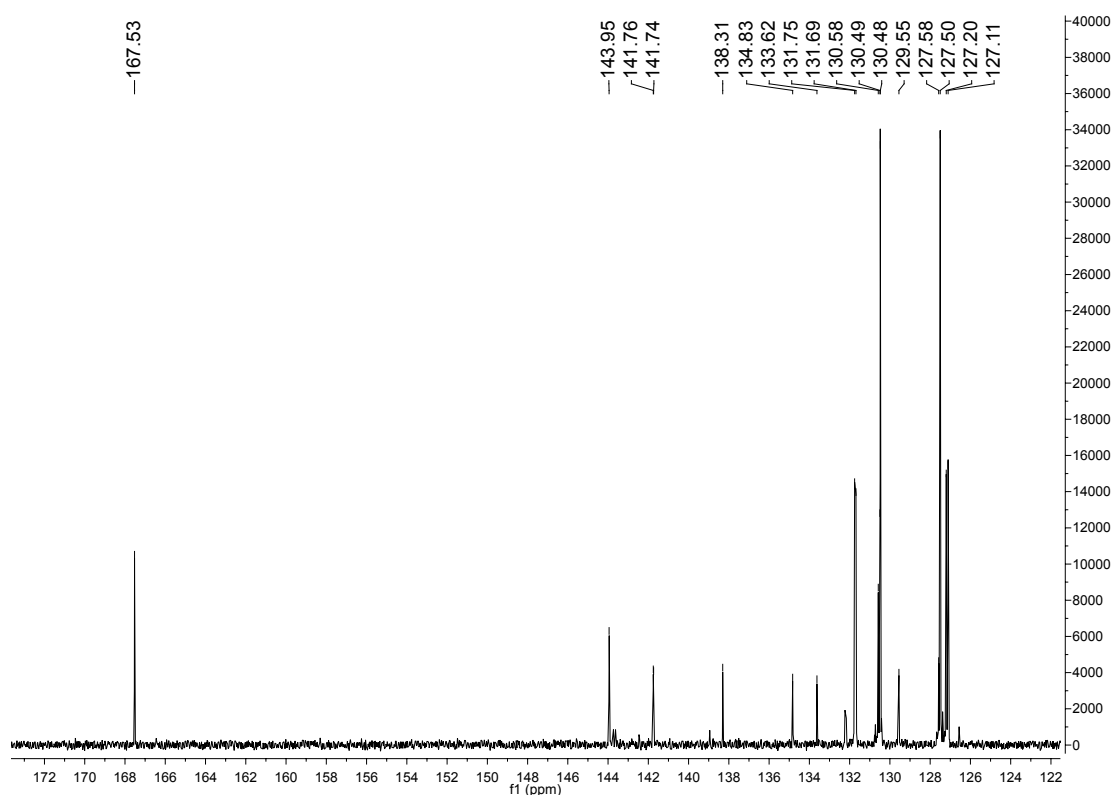


**Fig. S11**  $^{13}\text{C}$ -NMR spectrum of 4-phosphonato-4'-biphenylcarboxylic acid, **4** at 125.7 MHz in  $\text{DMSO}-d_6$ .

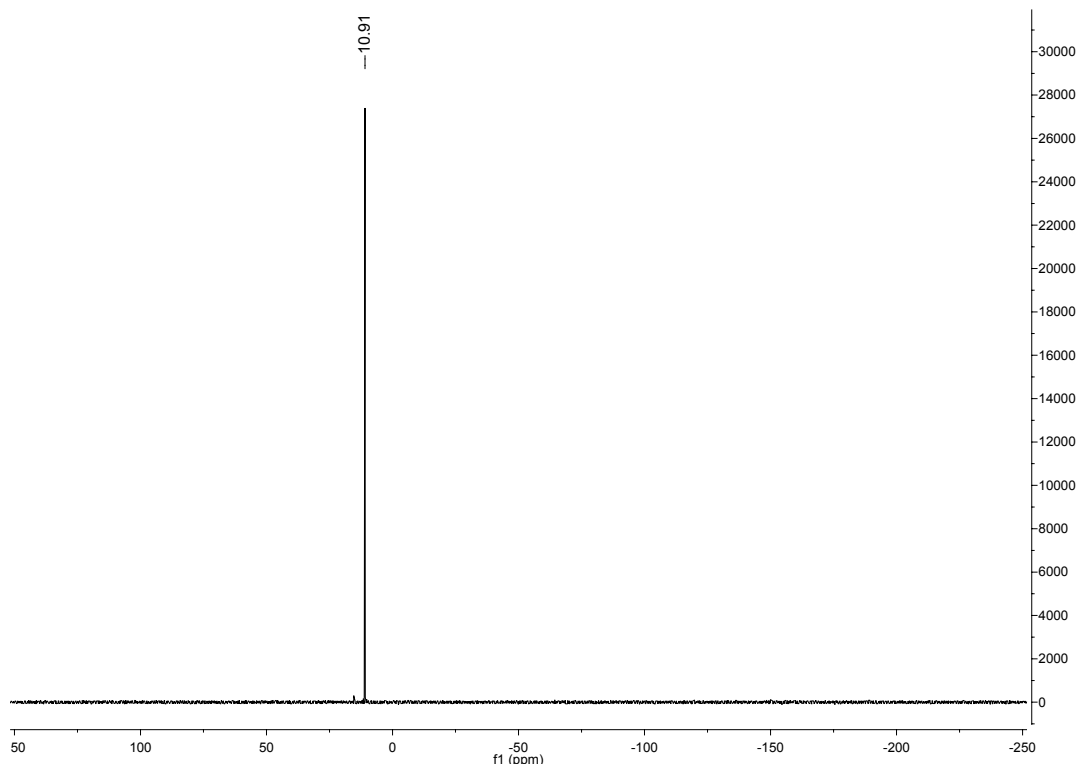


**Fig. S12**  $^{31}\text{P}\{\text{H}\}$ -NMR spectrum of 4-phosphonato-4'-biphenylcarboxylic acid, **4** at 121.5 MHz in 25%  $\text{ND}_3$  in  $\text{D}_2\text{O}$ .

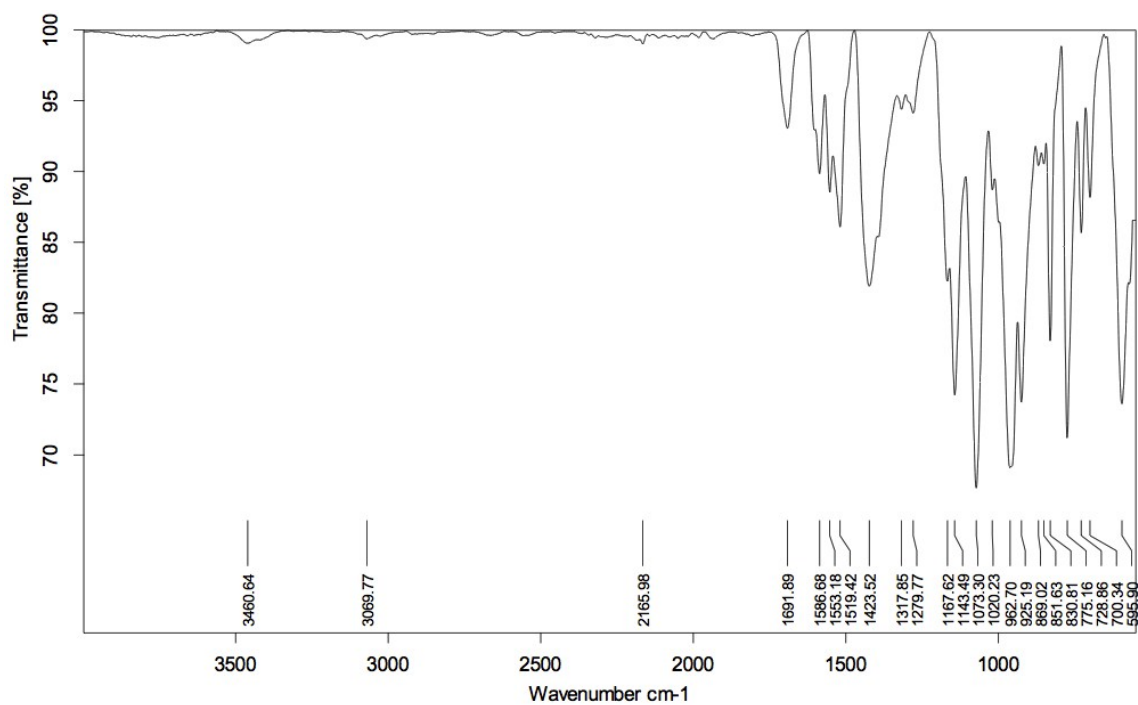


**Fig. S13** FT-IR (ATR) spectrum of  $[\text{Zn}_5(\mu_3\text{-OH})_4(\mu_4\text{-O}_3\text{P-(C}_6\text{H}_4)_2\text{-CO}_2\text{-}\mu_2)_2]$ , **5**.

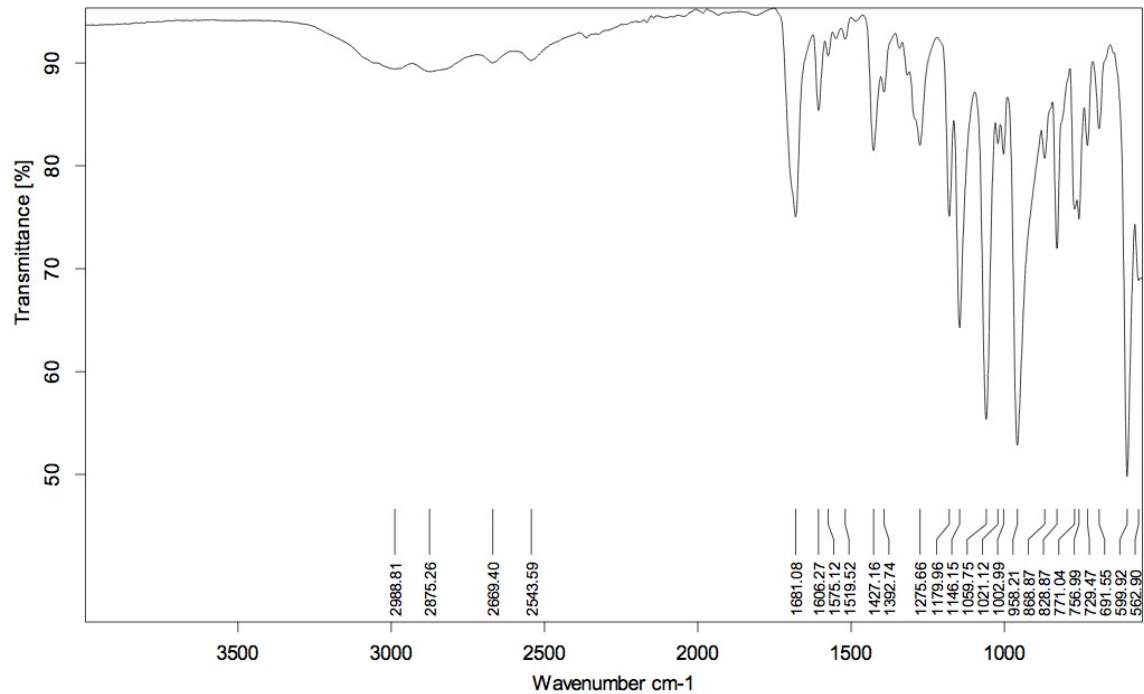


**Fig. S14** FT-IR(ATR) spectrum of  $[\text{Zn}(\mu_6\text{-O}_3\text{P-(C}_6\text{H}_4)_2\text{-CO}_2\text{H})]$ , **6**.

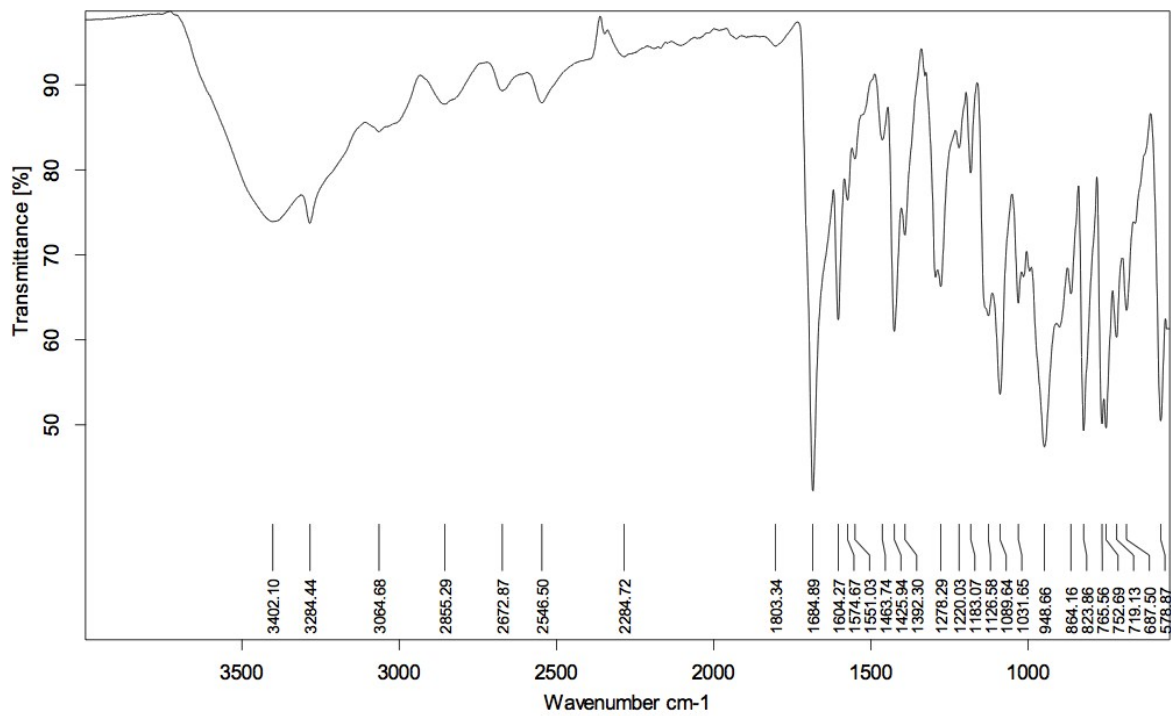


**Fig. S15** FT-IR (ATR) spectrum of  $[\text{Cd}_3(\mu_6\text{-O}_3\text{P}\text{-(C}_6\text{H}_4\text{)}_2\text{-CO}_2\text{-}\mu_2)\text{)(}\mu_6\text{-O}_3\text{P}\text{-(C}_6\text{H}_4\text{)}_2\text{-CO}_2\text{-}\mu_3\text{)]}, \mathbf{7}$ .

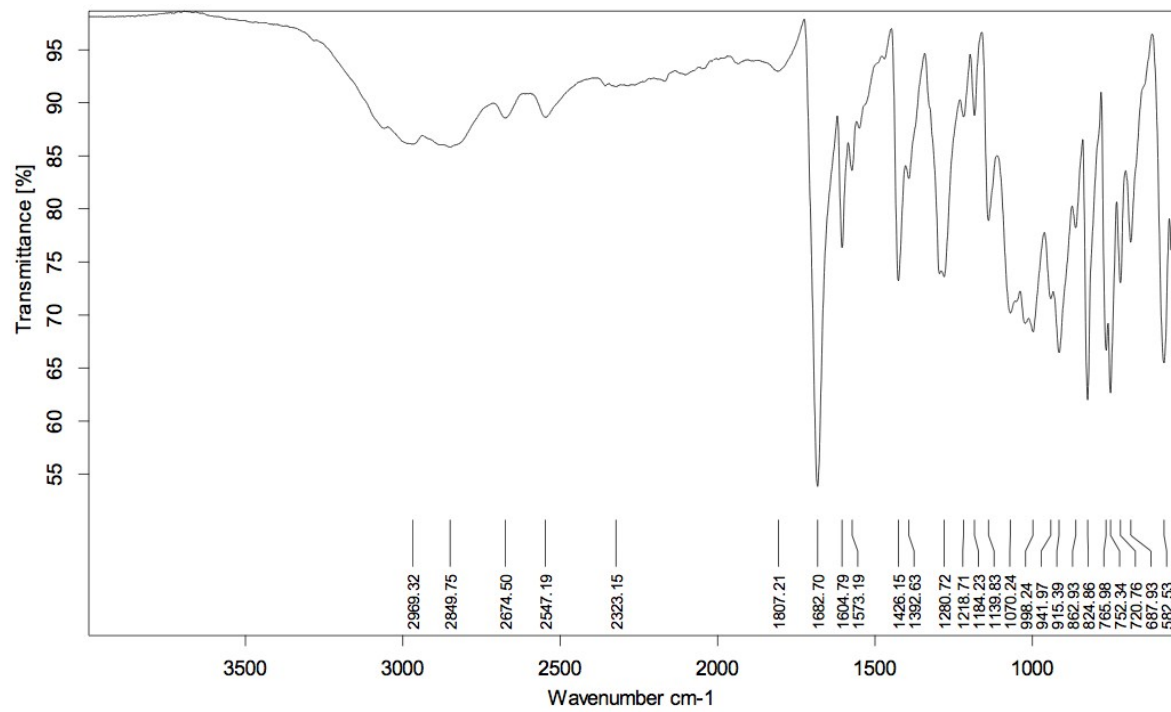


**Fig. S16** FT-IR (ATR) spectrum of  $[\text{Hg}(\mu_3\text{-HO}_3\text{P}\text{-(C}_6\text{H}_4\text{)}_2\text{-CO}_2\text{H})], \mathbf{8}$ .

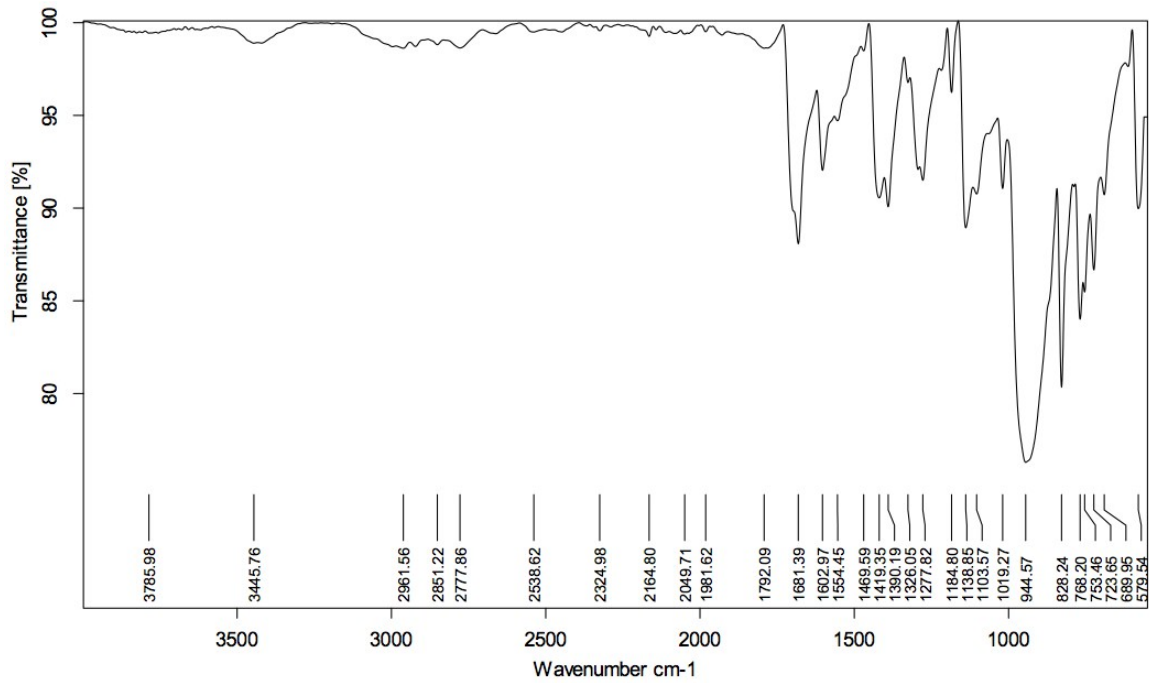


**Fig. S17** FT-IR (ATR) spectrum of  $[\text{Co}(\mu_6\text{-O}_3\text{P}\text{-(C}_6\text{H}_4\text{)}_2\text{-CO}_2\text{H})]$ , **9**.

### Thermogravimetric measurements

TG /%

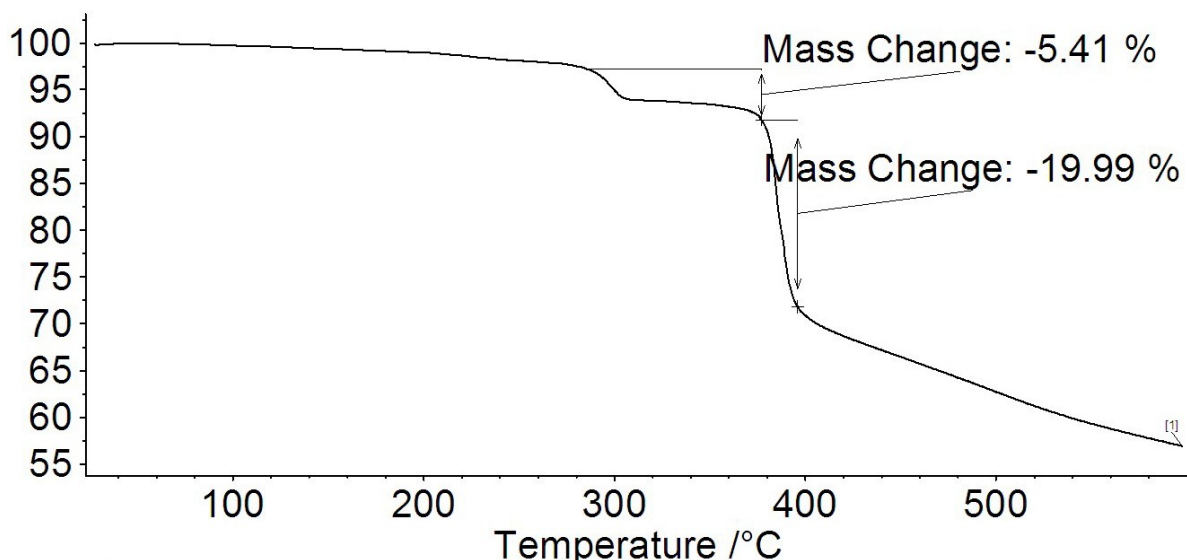


Fig. S18 TGA curve of 4-phosphonato-4'-biphenylcarboxylic acid, 4.

TG /%

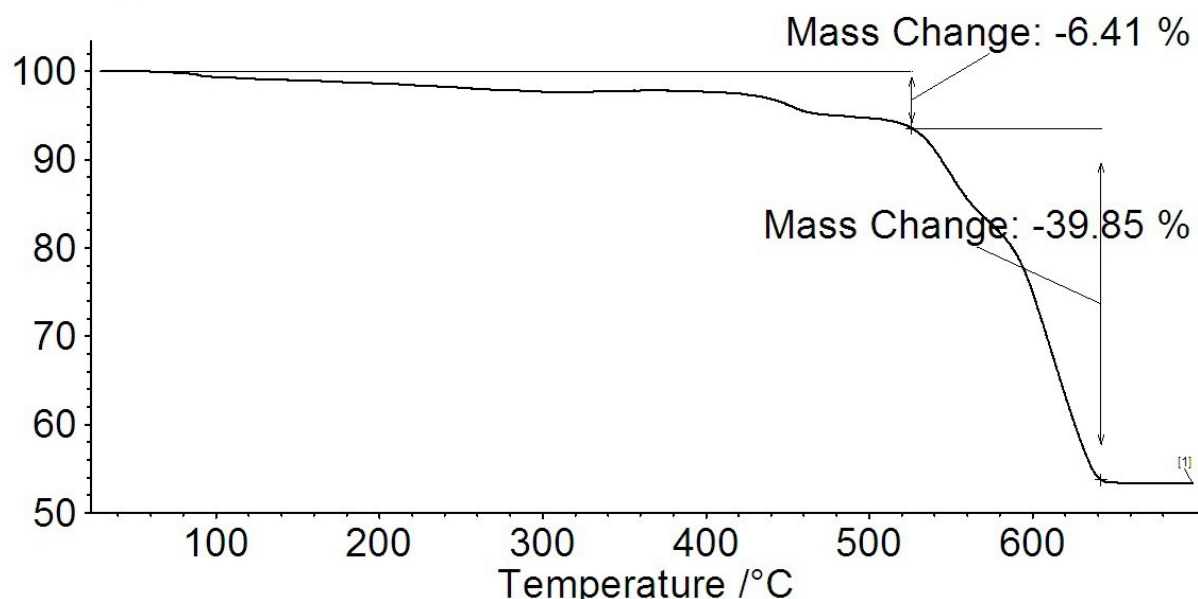
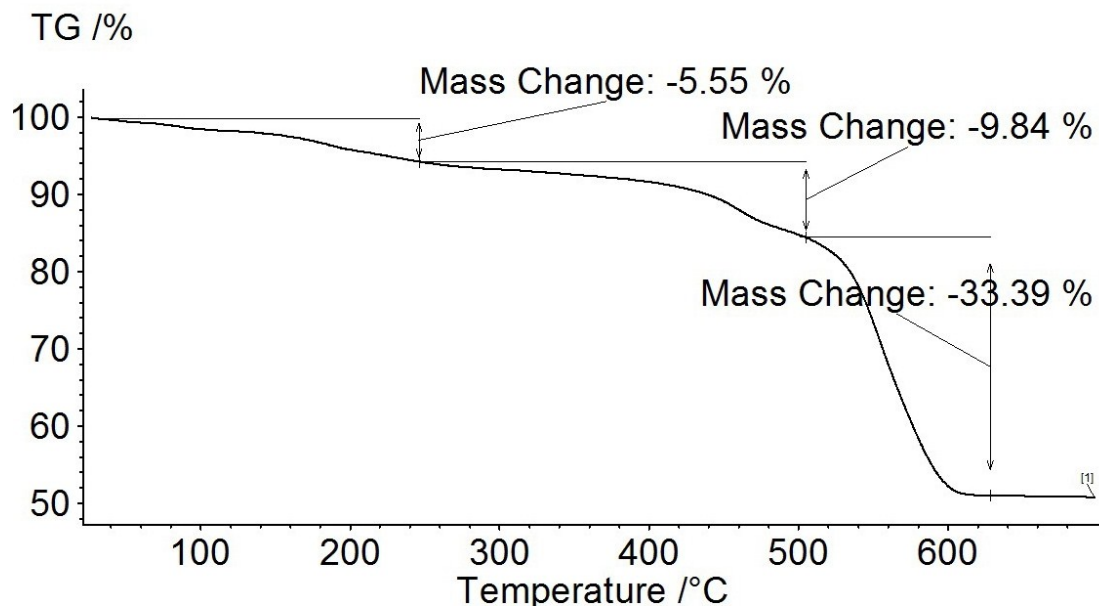
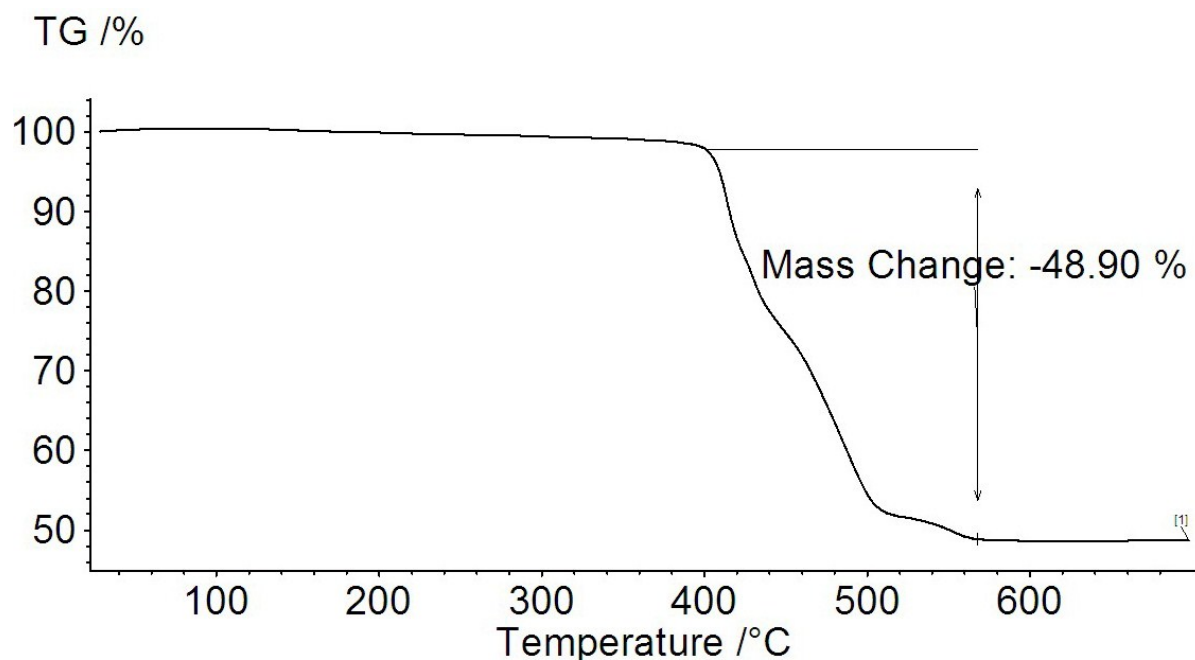


Fig. S19 TGA curve of  $[Zn_5(\mu_3-OH)_4(\mu_4-O_3P-(C_6H_4)_2-CO_2-\mu_2)_2]$ , 5.



**Fig. S20** TGA curve of  $[\text{Zn}(\mu_6\text{-O}_3\text{P-(C}_6\text{H}_4)_2\text{-CO}_2\text{H})]$ , **6**.



**Fig. S21** TGA curve of  $[\text{Cd}_3(\mu_6\text{-O}_3\text{P-(C}_6\text{H}_4)_2\text{-CO}_2\text{-}\mu_2)(\mu_6\text{-O}_3\text{P-(C}_6\text{H}_4)_2\text{-CO}_2\text{-}\mu_3)]$ , **7**.

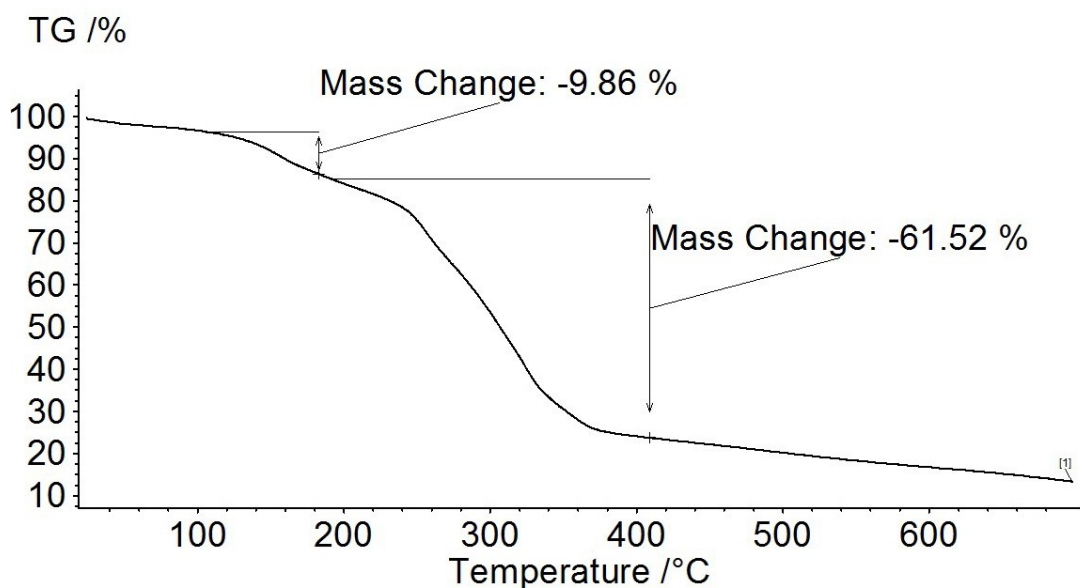


**Fig. S22** TGA curve of  $[\text{Hg}(\mu_3\text{-HO}_3\text{P-(C}_6\text{H}_4\text{)}_2\text{-CO}_2\text{H})]$ , **8**.

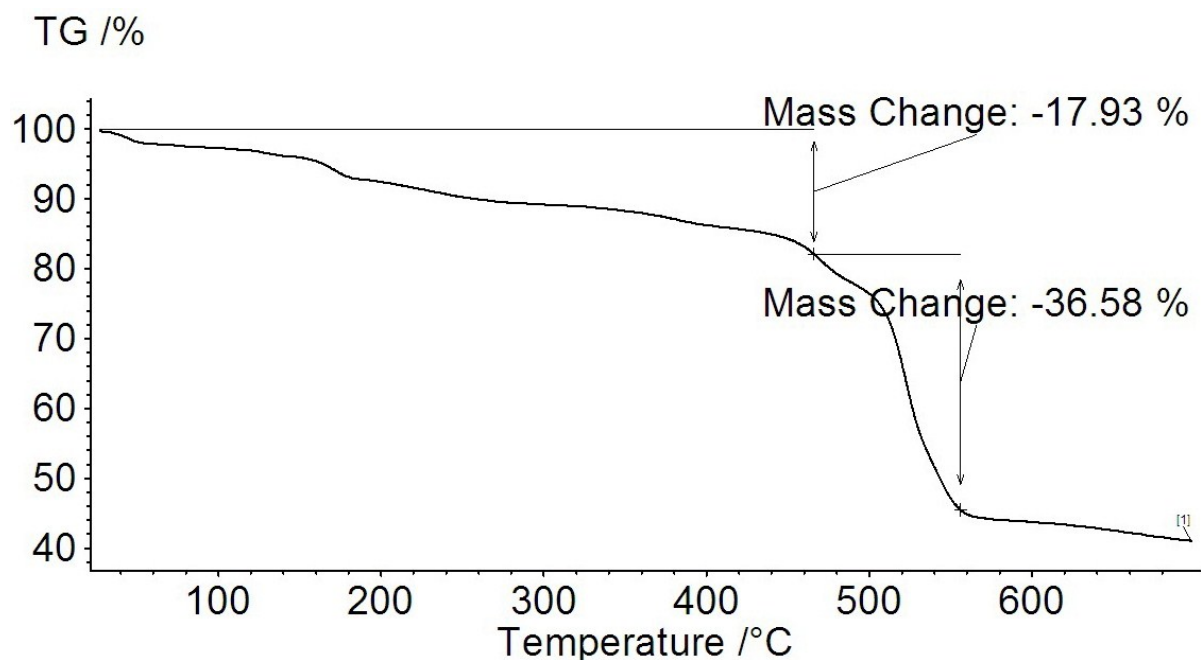


**Fig. S23** TGA curve of  $[\text{Co}(\mu_6\text{-O}_3\text{P-(C}_6\text{H}_4\text{)}_2\text{-CO}_2\text{H})]$ , **9**.

## Powder X-ray diffraction

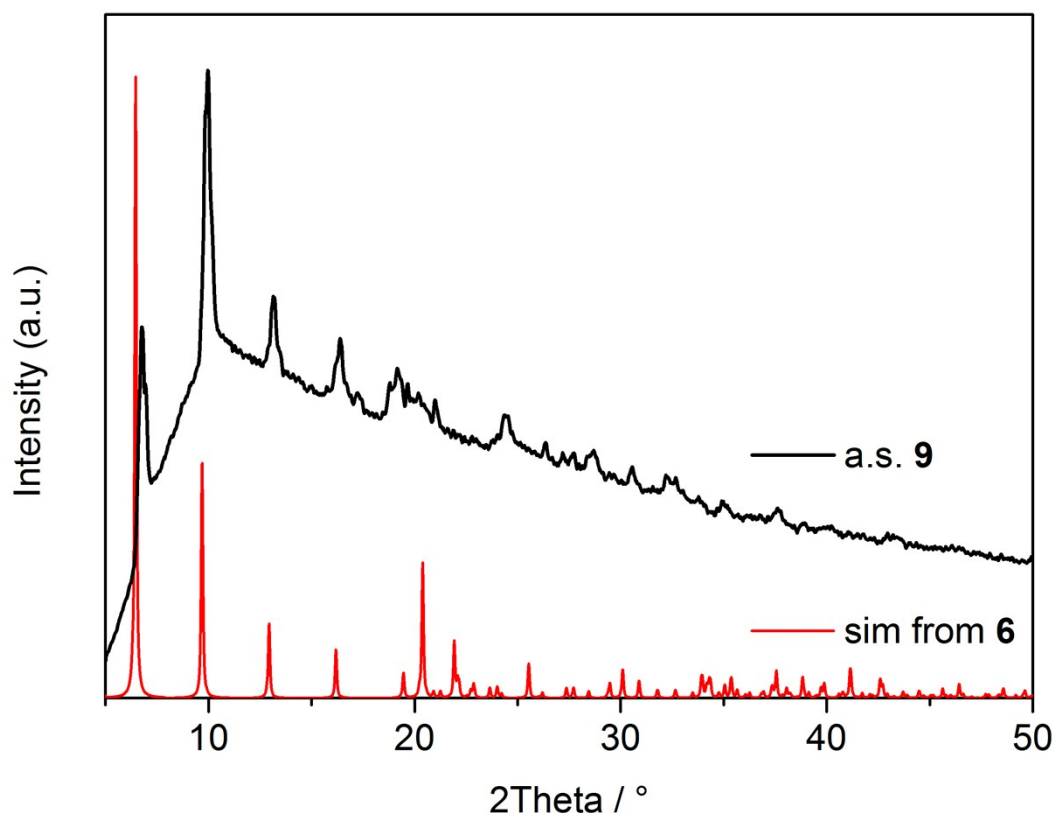


**Fig. S24** PXRD comparison of **6** (red, simulated from single-crystal X-ray data set, SCXRD) and **9** (black, as synthesized, a.s.) for demonstration of isostructural relation. The strong background for the a.s. sample is due to the fluorescence of Co(II) ions towards CuK $\alpha$  radiation.<sup>12</sup>.

12 A. R. West: "Solid State Chemistry and Its Applications" John Wiley & Sons, 1987, p 177.

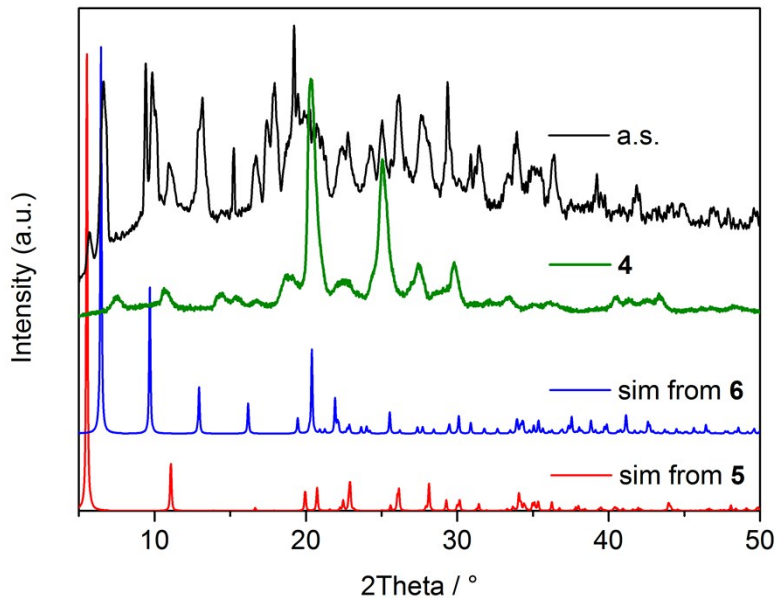


**Fig. S25** PXRD comparison of **5** and **6**. The pattern of "5" obtained after synthesis (black) with the simulated patterns of **5** and **6** (red and blue, respectively, from SCXRD). The green pattern is the experimental pattern of the crystalline powder of the  $\text{H}_3\text{BPPA}$  ligand **4**.

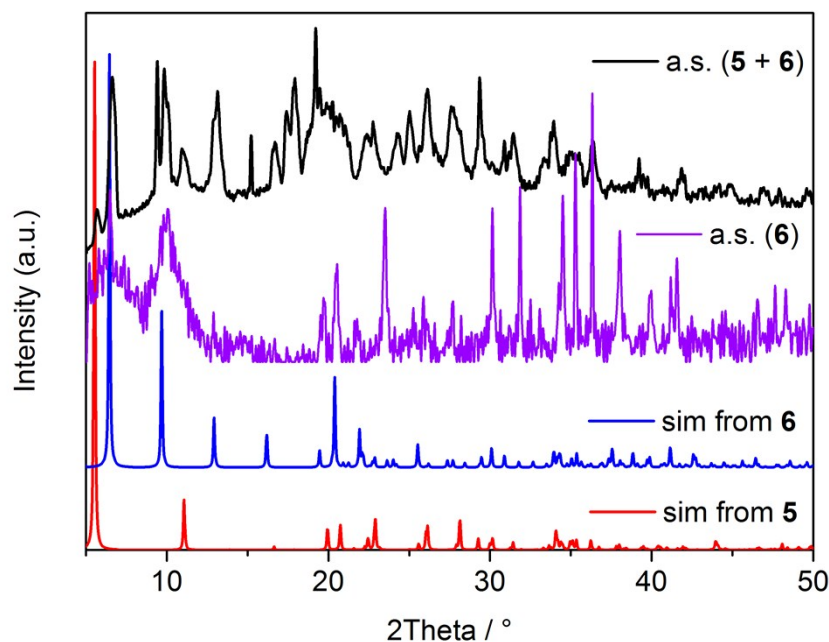


**Fig. S26** PXRD comparison of **5** and **6**. The pattern of "5" obtained after synthesis (black) with the simulated patterns of **5** and **6** (red and blue, respectively, from SCXRD) and the experimental pattern of **6** (purple, as synthesized, a.s.).

## Additional structure graphics

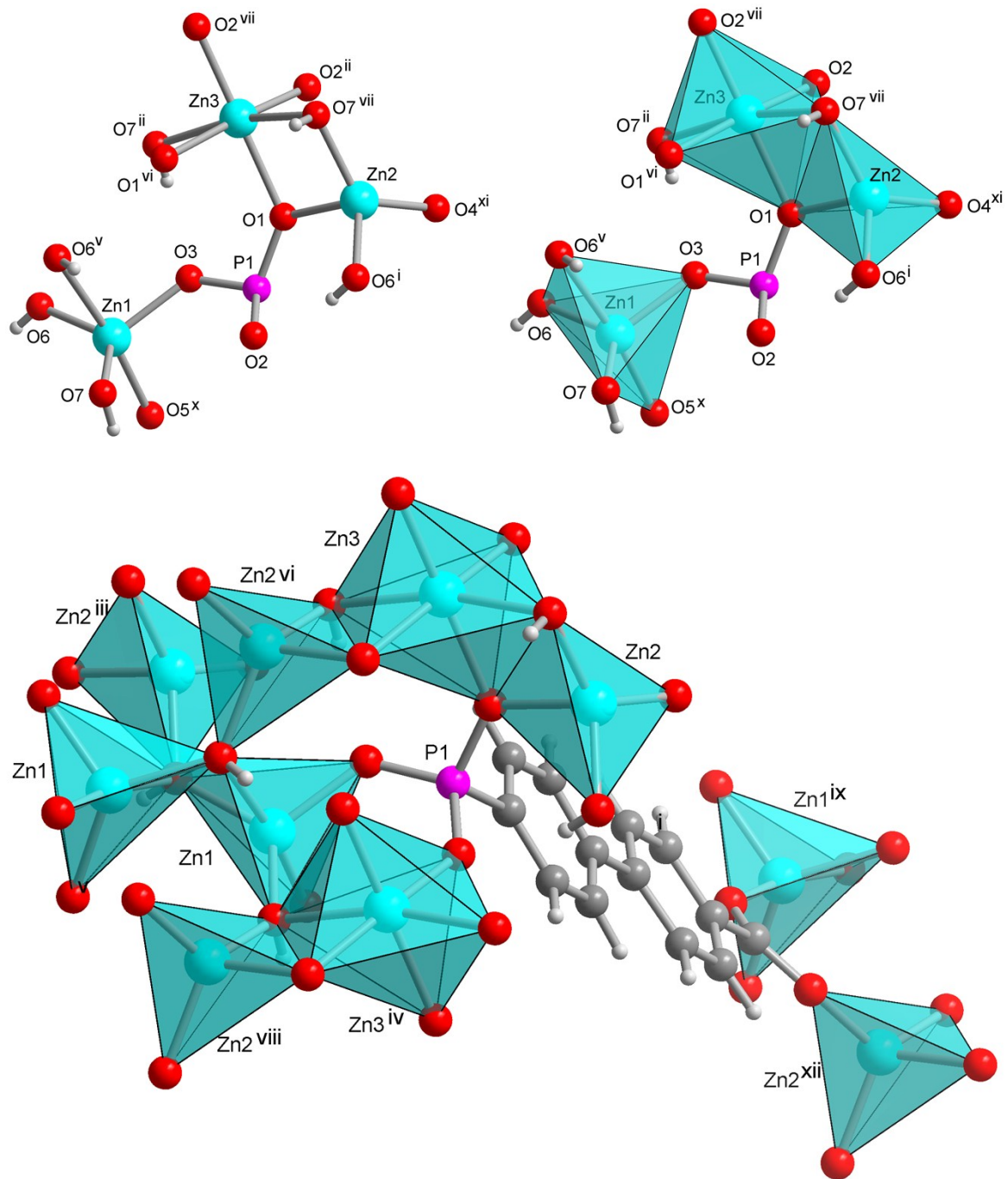


**Fig. S27** Coordination sphere around the crystallographic different Zn atoms 1, 2 and 3 in **5**. Hydrogen bonds from OH are depicted in Fig. S29.  
 Symmetriy transformations: i = x, y, 1+z; ii = x, 1+y, z; iii = x, y, -1+z; iv = x, -1+y, z; v = -x, y, -z; vi = -x, y, 1-z; vii = -x, 1+y, 1-z; viii = -x, -1+y, 1-z; ix = 0.5-x, 0.5+y, 1-z; x = 0.5-x, -0.5+y, 1-z; xi = 0.5-x, 0.5+y, 2-z; xii = 0.5-x, -0.5+y, 2-z.

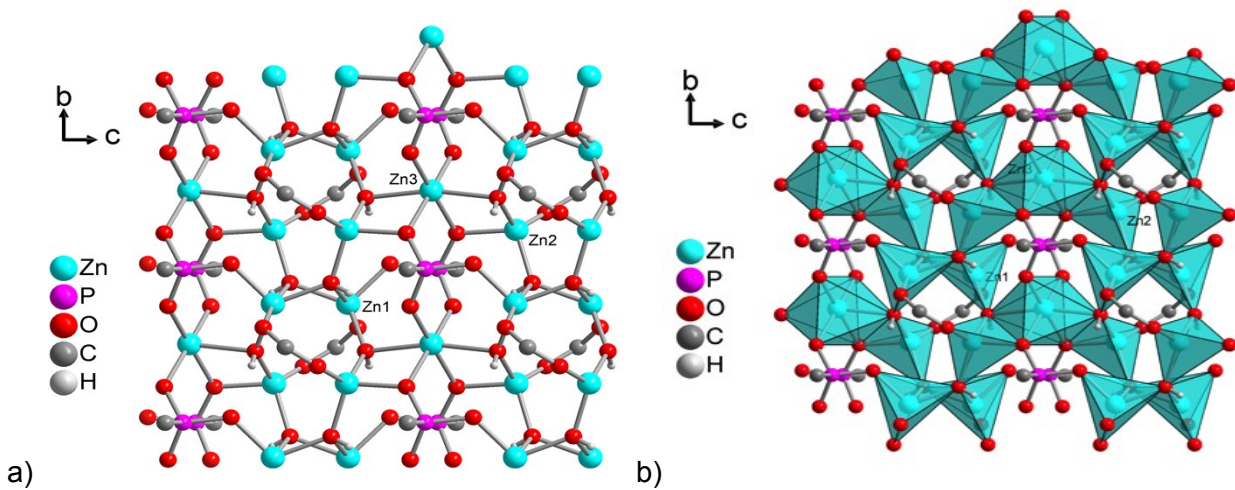


**Fig. S28** Ball-and-stick drawing of the  $\text{ZnO}$ -layer along  $a$ -axis (a) and with  $\text{ZnO}_x$  polyhedra (b) of complex **5**.

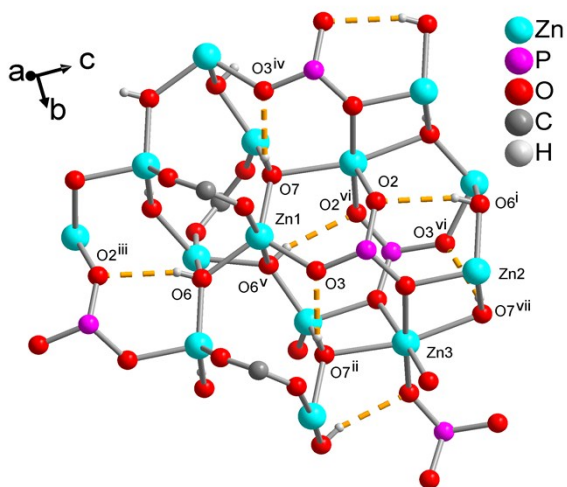


**Fig. S29** Hydrogen bonds from  $\text{OH}^-$  to phosphonato group in **5**. For details of the H-bonds see Table S5. Symmetry transformations  $i = x, 1+y, z$ ;  $\text{iii} = -x, 1+y, 1-z$ ;  $\text{iv} = 0.5-x, 0.5+y, 1-z$ ;  $v = 0.5+x, 0.5+y, 1+z$ ;  $\text{vi} = 0.5-x, 1.5+y, 1-z$ ;  $\text{vii} = x, y-1, z$ .

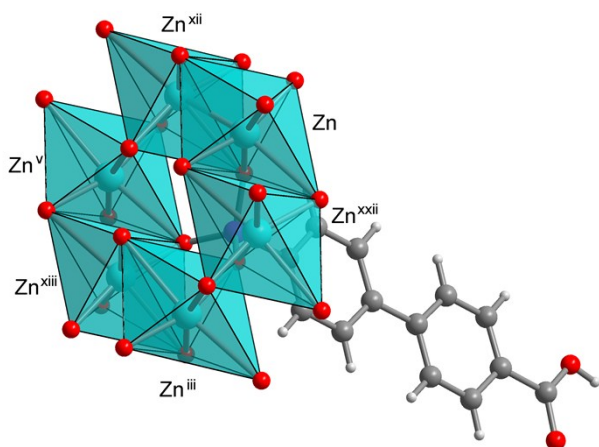


**Fig. S30** Expanded asymmetric unit of **6** with  $\{\text{ZnO}_6\}$  octahedra. Symmetry transformations  $\text{iii}: 1-x, y, 1-z$ ,  $\text{v}: 3/2-x, 1/2+y, 1-z$ ,  $\text{xii}: 1-x, 1+y, 1-z$ ,  $\text{xiii}: 1-x, 2-y, 1-z$ ,  $\text{xxii}: -x, 1-y, 1-z$ .

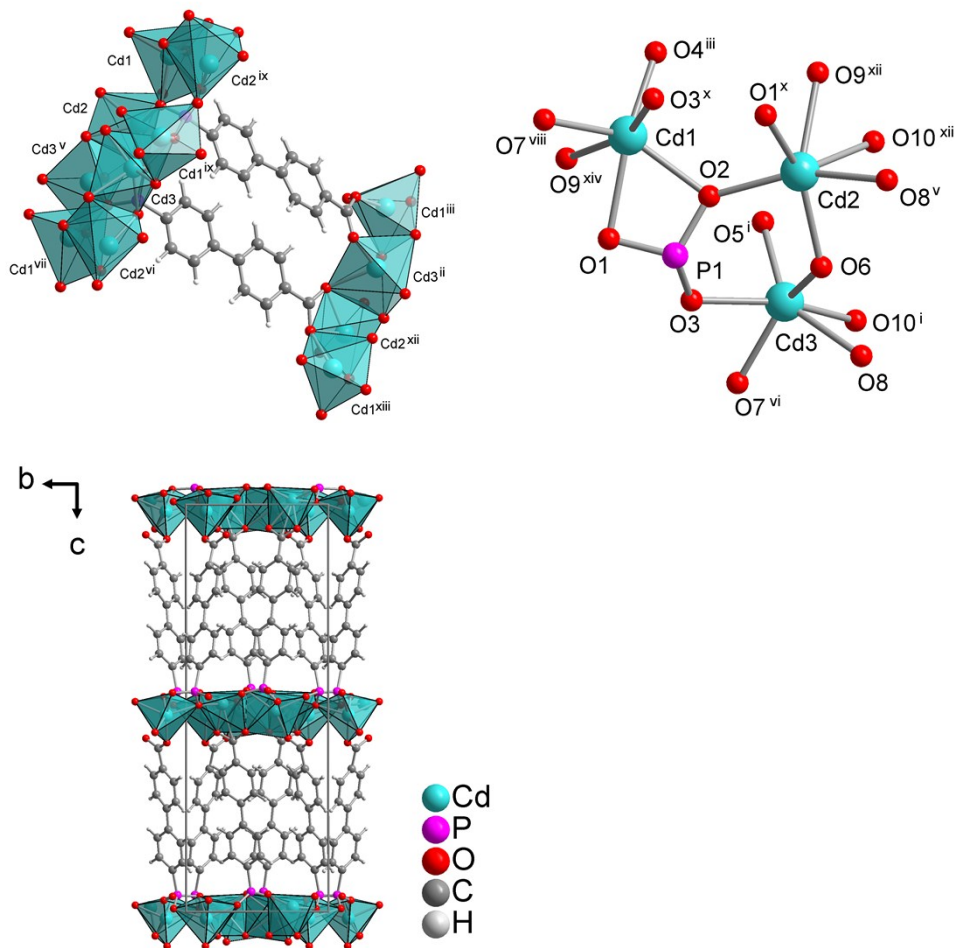


**Fig. S31** Expanded asymmetric unit of **7** with drawing of ball-and-stick model and  $\text{CdO}_x$  polyhedra highlighted(left). Coordination sphere around the crystallographic different Cd atoms 1, 2 and 3 in **7** (right). Symmetry transformations i:  $1/2-x, y, 1/2+z$ , ii:  $1/2-x, y, -1/2+z$ , iii:  $-x, 2-y, 1/2+z$ , v:  $-1/2+x, 1-y, z$ , vi:  $1/2+x, 1-y, z$ , vii:  $x, -1+y, z$ , ix:  $1/2+x, 2-y, z$ , x:  $-1/2+x, 2-y, z$ , xii:  $-x, 1-y, 1/2+z$ , xiii:  $1/2-x, -1+y, -1/2+z$ , xiv:  $1/2-x, 1+y, 1/2+z$ .

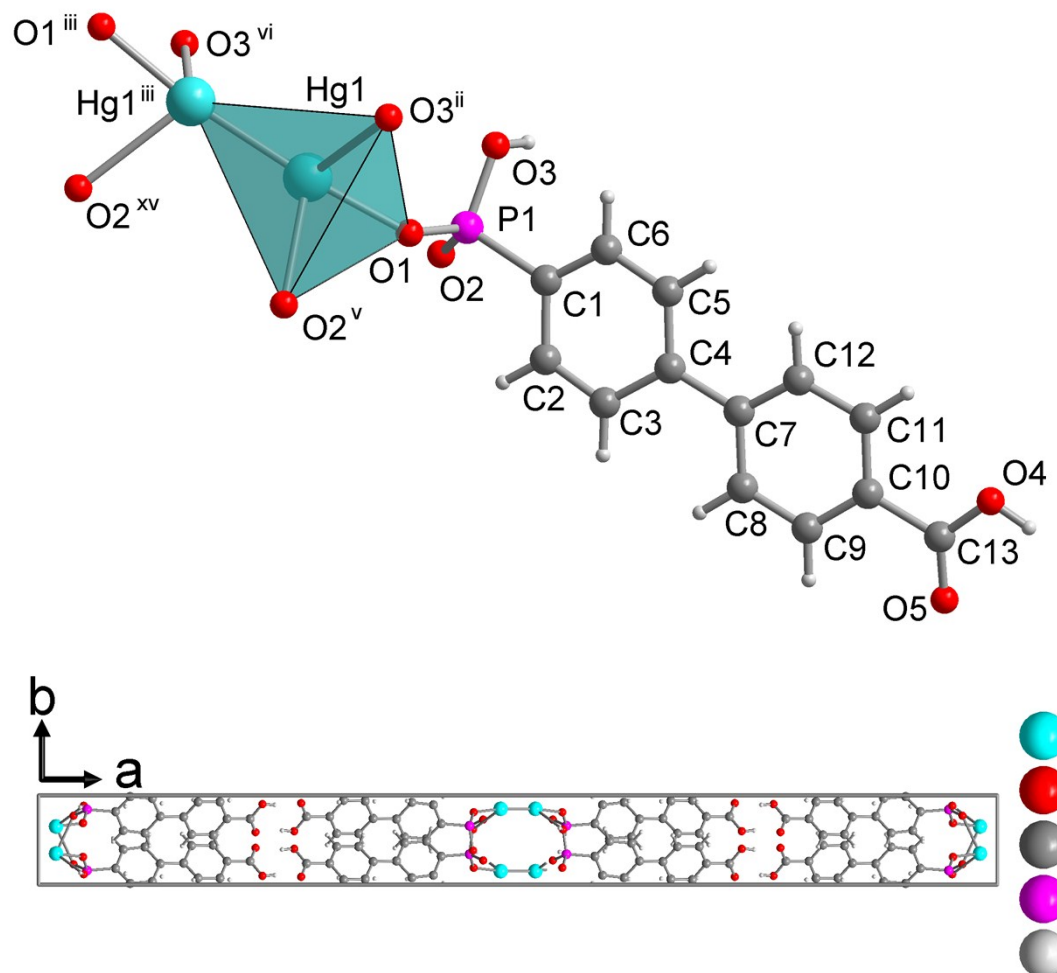


**Fig. S32** Top: Expanded asymmetric unit of **8** with drawing of ball-and-stick model and  $\text{Hg}_2\text{O}_3$  polyhedra highlighted. Bottom: Projection of the packing diagram on the  $ab$  plane. Symmetry transformations ii:  $+x, 1-y, -1/2+z$ , iii:  $1-x, +y, 1/2-z$ , v:  $+x, -y, -1/2+z$ , vi:  $1-x, 1-y, 1-z$ , xv:  $1-x, -y, 1-z$ .

## Structure Tables

Tables were created with publCIF.<sup>13</sup>

**Table S1** Bond lengths and angles (Å, °) for **2**.

I1—C1	2.082(9)	C8—C9	1.375(12)
C1—C2	1.383(12)	C8—C7	1.405(11)
C1—C6	1.400(13)	C13—C10	1.490(13)
O1—C13	1.202(13)	C10—C11	1.395(12)
C2—C3	1.379(15)	C10—C9	1.398(12)
O2—C13	1.303(12)	C11—C12	1.377(12)
O2—C14	1.440(18)	C12—C7	1.409(11)
C3—C4	1.397(13)	C5—C4	1.390(10)
C5—C6	1.376(12)	C4—C7	1.484(12)
C2—C1—C6	118.4(8)	C9—C8—C7	122.5(8)
C2—C1—I1	121.2(7)	C11—C10—C9	118.1(8)
C6—C1—I1	120.4(6)	C11—C10—C13	119.0(8)
C3—C2—C1	120.3(8)	C9—C10—C13	122.9(8)
C13—O2—C14	117.9(10)	C2—C3—C4	122.2(7)
C5—C4—C3	116.7(8)	C6—C5—C4	121.7(8)
C5—C4—C7	121.2(7)	O1—C13—O2	123.6(10)
C3—C4—C7	122.1(7)	O1—C13—C10	123.4(9)
C5—C6—C1	120.6(7)	O2—C13—C10	112.9(8)
C8—C9—C10	120.7(8)	C11—C12—C7	122.3(6)
C12—C11—C10	120.8(7)	C8—C7—C12	115.7(8)
C6—C1—C2—C3	1.5(12)	C8—C7—C4	122.2(7)
I1—C1—C2—C3	-179.3(7)	C12—C7—C4	122.1(7)
C1—C2—C3—C4	-0.5(14)	C12—C7—C4	122.1(7)

13 S. P. Westrip, *J. Appl. Cryst.*, 2010, **43**, 920-925.

C6—C5—C4—C3	0.6(11)	O2—C13—C10—C9	-6.7(10)
C6—C5—C4—C7	-178.2(7)	C7—C8—C9—C10	-0.4(11)
C2—C3—C4—C5	-0.6(12)	C11—C10—C9—C8	0.0(11)
C2—C3—C4—C7	178.3(8)	C13—C10—C9—C8	178.8(7)
C4—C5—C6—C1	0.4(13)	C9—C10—C11—C12	0.5(12)
C2—C1—C6—C5	-1.4(12)	C13—C10—C11—C12	-178.4(7)
I1—C1—C6—C5	179.3(6)	C10—C11—C12—C7	-0.5(12)
C14—O2—C13—O1	2.2(14)	C9—C8—C7—C12	0.4(11)
C14—O2—C13—C10	-175.8(8)	C9—C8—C7—C4	-179.9(6)
O1—C13—C10—C11	-5.9(12)	C11—C12—C7—C8	0.1(11)
O2—C13—C10—C11	172.2(7)	C11—C12—C7—C4	-179.6(7)
O1—C13—C10—C9	175.3(9)	C5—C4—C7—C8	179.7(7)
C3—C4—C7—C8	0.9(10)		

**Table S2** Bond lengths and angles ( $\text{\AA}$ ,  $^\circ$ ) for **3**.

P1—O2	1.462(2)	C5—C6	1.384(4)
P1—O1	1.560(2)	O5—C13	1.195(3)
P1—O3	1.567(2)	C7—C12	1.394(3)
P1—C1	1.788(3)	C7—C8	1.397(4)
O1—C15	1.446(4)	C8—C9	1.380(4)
O4—C13	1.341(3)	C1—C6	1.400(3)
O4—C14	1.449(3)	C2—C3	1.378(4)
C1—C2	1.387(4)	C9—C10	1.395(4)
C3—C4	1.403(3)	C10—C11	1.388(4)
O3—C17	1.437(5)	C10—C13	1.494(4)
C4—C5	1.397(4)	C11—C12	1.389(4)
C4—C7	1.481(4)	C6—C5—C4	121.0(2)
C16—C15	1.486(4)	C5—C6—C1	120.6(2)

C18—C17	1.338(7)	C12—C7—C8	117.9(2)
O2—P1—O1	116.11(13)	C12—C7—C4	121.3(2)
O2—P1—O3	113.98(13)	C8—C7—C4	120.8(2)
O1—P1—O3	102.44(13)	C9—C8—C7	121.9(2)
O2—P1—C1	113.48(13)	C8—C9—C10	119.7(2)
O1—P1—C1	101.48(11)	C11—C10—C9	119.2(2)
O3—P1—C1	108.04(11)	C11—C10—C13	122.8(2)
C15—O1—P1	121.6(2)	C9—C10—C13	117.9(2)
C13—O4—C14	115.3(2)	O5—C13—O4	123.5(2)
C2—C1—C6	118.4(2)	O5—C13—C10	124.4(2)
C2—C1—P1	118.48(18)	O4—C13—C10	112.2(2)
C6—C1—P1	123.1(2)	C10—C11—C12	120.7(2)
C3—C2—C1	121.3(2)	C11—C12—C7	120.7(2)
C2—C3—C4	120.8(2)	C18—C17—O3	115.5(5)
C17—O3—P1	122.1(3)	P1—C1—C6—C5	179.36(19)
C5—C4—C3	117.9(2)	C5—C4—C7—C12	-36.2(3)
C5—C4—C7	121.7(2)	C3—C4—C7—C12	144.3(2)
C3—C4—C7	120.4(2)	C5—C4—C7—C8	144.6(2)
O1—C15—C16	107.6(3)	C3—C4—C7—C8	-34.9(3)
O2—P1—O1—C15	-46.8(3)	C12—C7—C8—C9	0.1(4)
O3—P1—O1—C15	78.1(3)	C4—C7—C8—C9	179.4(2)
C1—P1—O1—C15	-170.3(3)	C7—C8—C9—C10	0.0(4)
O2—P1—C1—C2	-23.6(3)	C8—C9—C10—C11	-0.3(4)
O1—P1—C1—C2	101.7(2)	C8—C9—C10—C13	179.8(2)
O3—P1—C1—C2	-151.0(2)	C14—O4—C13—O5	-0.7(4)
O2—P1—C1—C6	156.8(2)	C14—O4—C13—C10	178.8(2)
O1—P1—C1—C6	-77.9(2)	C11—C10—C13—O5	-166.8(2)
O3—P1—C1—C6	29.4(2)	C9—C10—C13—O5	13.1(4)
C6—C1—C2—C3	1.2(4)	C11—C10—C13—O4	13.8(3)

P1—C1—C2—C3	-178.4(2)	C9—C10—C13—O4	-166.3(2)
C1—C2—C3—C4	-1.6(4)	C9—C10—C11—C12	0.5(4)
O2—P1—O3—C17	-37.5(3)	C13—C10—C11—C12	-179.6(2)
O1—P1—O3—C17	-163.7(3)	C10—C11—C12—C7	-0.4(4)
C1—P1—O3—C17	89.7(3)	C8—C7—C12—C11	0.1(3)
C2—C3—C4—C5	1.0(4)	C4—C7—C12—C11	-179.1(2)
C2—C3—C4—C7	-179.4(2)	P1—O3—C17—C18	-104.0(6)
P1—O1—C15—C16	160.8(2)	C4—C5—C6—C1	-0.3(4)
C3—C4—C5—C6	-0.1(4)	C2—C1—C6—C5	-0.2(4)
C7—C4—C5—C6	-179.6(2)		

**Table S3.** Hydrogen-bond geometry ( $\text{\AA}$ ,  $^\circ$ ) for **3**.

$D—H\cdots A$	$D—H$	$H\cdots A$	$D\cdots A$	$D—H\cdots A$
C17—H17A $\cdots$ O2	0.97	2.56	3.039(5)	111
C17—H17B $\cdots$ O5 <sup>i</sup>	0.97	2.56	3.507(7)	164

Symmetry code: i = x-1, y, z-1.

**Table S4** Hydrogen-bond geometry ( $\text{\AA}$ ,  $^\circ$ ) for **5**.

$D-\text{H}\cdots A$	$D-\text{H}$	$\text{H}\cdots A$	$D\cdots A$	$D-\text{H}\cdots A$
O6—H1···O2 <sup>xi</sup>	0.76 (11)	2.17 (11)	2.860 (6)	150 (12)
O6—H1···O7 <sup>ii</sup>	0.76(11)	2.34 (12)	2.845 (7)	125 (11)
O7—H7···O3 <sup>viii</sup>	0.79 (8)	2.03 (7)	144 (7)	144 (7)

Symmetry codes: ii = x, 1+y, z; ; viii = -x, -1+y, 1-z;; xi = 0.5-x, 0.5+y, 2-z.

**Table S5** Hydrogen-bond geometry ( $\text{\AA}$ ,  $^\circ$ ) for **6**.

$D-\text{H}\cdots A$	$D-\text{H}$	$\text{H}\cdots A$	$D\cdots A$	$D-\text{H}\cdots A$
O3—H3A···O4 <sup>xiii</sup>	0.83(1)	1.77(1)	2.61(2)	170.90(8)

Symmetry transformation: xiii = 2-x, 1-y, -z.

**Table S6** Selected angles ( $^{\circ}$ ) for 7.

O4 <sup>iii</sup> —Cd1—O7 <sup>vii</sup>	108.8(4)	O2—Cd2—O8 <sup>vi</sup>	157.5(3)
O4 <sup>iii</sup> —Cd1—O2	106.6(4)	O2—Cd2—O1 <sup>x</sup>	92.7(3)
O7 <sup>vii</sup> —Cd1—O2	139.4(3)	O8 <sup>vi</sup> —Cd2—O1 <sup>x</sup>	88.1(3)
O4 <sup>iii</sup> —Cd1—O3 <sup>x</sup>	89.7(3)	O2—Cd2—O6	83.2(3)
O7 <sup>vii</sup> —Cd1—O3 <sup>x</sup>	71.0(3)	O8 <sup>vi</sup> —Cd2—O6	82.9(3)
O2—Cd1—O3 <sup>x</sup>	90.3(3)	O1 <sup>x</sup> —Cd2—O6	143.7(3)
O4 <sup>iii</sup> —Cd1—O1	158.0(3)	O2—Cd2—O9 <sup>xii</sup>	107.1(3)
O7 <sup>vii</sup> —Cd1—O1	88.3(3)	O5 <sup>i</sup> —Cd3—O7 <sup>v</sup>	117.0(4)
O2—Cd1—O1	63.9(3)	O5 <sup>i</sup> —Cd3—O6	102.6(4)
O3 <sup>x</sup> —Cd1—O1	109.5(3)	O7 <sup>v</sup> —Cd3—O6	134.4(3)
O4 <sup>iii</sup> —Cd1—O9 <sup>xiv</sup>	91.5(3)	O5 <sup>i</sup> —Cd3—O3	89.3(3)
O7 <sup>vii</sup> —Cd1—O9 <sup>xiv</sup>	88.3(3)	O7 <sup>v</sup> —Cd3—O3	72.6(3)
O2—Cd1—O9 <sup>xiv</sup>	110.0(3)	O6—Cd3—O3	86.9(3)
O3 <sup>x</sup> —Cd1—O9 <sup>xiv</sup>	158.4(3)	O5 <sup>i</sup> —Cd3—O8	144.2(3)
O1—Cd1—O9 <sup>xiv</sup>	74.7(3)	O7 <sup>v</sup> —Cd3—O8	92.3(3)
O8 <sup>vi</sup> —Cd2—O9 <sup>xii</sup>	94.9(3)	O6—Cd3—O8	63.5(3)
O1 <sup>x</sup> —Cd2—O9 <sup>xii</sup>	76.6(3)	O3—Cd3—O8	120.6(3)
O6—Cd2—O9 <sup>xii</sup>	139.0(3)	O5 <sup>i</sup> —Cd3—O10 <sup>i</sup>	85.5(4)
O2—Cd2—O10 <sup>xii</sup>	119.3(3)	O7 <sup>v</sup> —Cd3—O10 <sup>i</sup>	87.7(3)
O8 <sup>vi</sup> —Cd2—O10 <sup>xii</sup>	77.2(3)	O6—Cd3—O10 <sup>i</sup>	118.5(3)
O1 <sup>x</sup> —Cd2—O10 <sup>xii</sup>	126.4(3)	O3—Cd3—O10 <sup>i</sup>	154.6(3)
O6—Cd2—O10 <sup>xii</sup>	85.7(3)	O8—Cd3—O10 <sup>i</sup>	74.9(3)
O9 <sup>xii</sup> —Cd2—O10 <sup>xii</sup>	54.3(3)		
		Cd2 <sup>xi</sup> —O10—Cd3 <sup>ii</sup>	95.5(3)
Cd2—O2—Cd1	126.7(3)	Cd2 <sup>xi</sup> —O9—Cd1 <sup>xiii</sup>	97.8(3)
Cd3—O3—Cd1 <sup>ix</sup>	86.8(3)	Cd3 <sup>v</sup> —O7—Cd1 <sup>ii</sup>	92.3(3)
Cd2 <sup>vi</sup> —O8—Cd3	106.5(3)	Cd2—O6—Cd3	119.0(3)

Symmetry transformations: i = 1/2-x, y, 1/2+z; ii = 1/2-x, y, -1/2+z; iii = -x, 2-y, 1/2+z; v = -

$1/2+x, 1-y, z$ ;  $vi = 1/2+x, 1-y, z$ ;  $vii = x, -1+y, z$ ;  $ix = 1/2+x, 2-y, z$ ;  $x = -1/2+x, 2-y, z$ ;  $xi = -x, 1-y, -1/2+z$ ;  $xii = -x, 1-y, 1/2+z$ ;  $xiii = 1/2-x, -1+y, -1/2+z$ ;  $xiv = 1/2-x, 1+y, 1/2+z$ .

**Table S7** Hydrogen-bond geometry ( $\text{\AA}$ ,  $^\circ$ ) for **7**.

$D-\text{H}\cdots A$	$D-\text{H}$		$\text{H}\cdots A$	$D\cdots A$	$D-\text{H}\cdots A$
C15—H15···O8 <sup>vi</sup>	0.95		2.61	3.262(17)	126

Symmetry transformation:  $vi = 1/2+x, 1-y, z$

**Table S8** Hydrogen-bond geometry ( $\text{\AA}$ ,  $^\circ$ ) for **8**.

$D-\text{H}\cdots A$	$D-\text{H}$	$\text{H}\cdots A$	$D\cdots A$	$D-\text{H}\cdots A$
O3—H3 $\cdots$ O2 <sup>iv</sup>	0.89(5)	1.67(10)	2.514(18)	158(21)
O4—H4 $\cdots$ O5 <sup>xiii</sup>	0.84	1.78	2.619(19)	174
C2—H2 $\cdots$ O1 <sup>iii</sup>	0.95	2.49	3.37(2)	154

Symmetry codes: <sup>iii</sup> =  $x$ ,  $-y$ ,  $-z+1/2$ ; <sup>iv</sup> =  $x$ ,  $1-y$ ,  $-1/2+z$ ; <sup>xiii</sup> =  $-x+1/2$ ,  $-y+1/2$ ,  $-z+2$ .

## Supramolecular Packing Analyses

Packing Analysis by PLATON((a) A. Spek, *Acta Crystallographica Section D*, 2009, **65**, 148-155;(b) A. L. Spek *PLATON – A multipurpose crystallographic tool*, Utrecht University: Utrecht, The Netherlands, 2005.)

Despite the presence of biphenyl  $\pi$ -systems in compounds **1** and **2**, there are no  $\pi\cdots\pi$  interactions<sup>14</sup> and only few intermolecular C-H $\cdots\pi$ <sup>15</sup> evident.

The supramolecular packing analyses of the biphenyl rings are tabulated below(Tables S12 – S14).

The listed "Analysis of Short Ring-Interactions" for possible  $\pi$ -stacking interactions yielded rather long centroid-centroid distances(>4.0 Å) together with non-parallel ring planes( $\alpha >> 0^\circ$ ) and large slip angles( $\beta, \gamma > 30^\circ$ ).

In comparison, significant  $\pi$ -stacking shows rather short centroid-centroid contacts(<3.8 Å), near parallel ring planes(alpha < 10° to ~0° or even exactly 0° by symmetry), small slip angles( $\beta, \gamma < 25^\circ$ ) and vertical displacements(slippage < 1.5 Å) which translate into a sizable overlap of the aryl-plane areas.<sup>4,16</sup>

Significant intermolecular C-H $\cdots\pi$  contacts start around 2.7 Å for the(C-)H $\cdots$ ring centroid distances with H-Perp also starting at 2.6-2.7 Å and C-H $\cdots$ Cg > 145°<sup>4,17,18</sup>

---

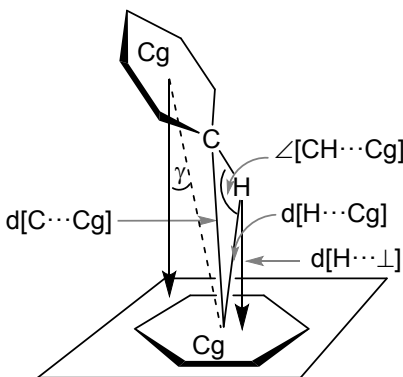
14 C. Janiak, *J. Chem. Soc., Dalton Trans.*, 2000, 3885-3896.

15 M. Nishio, *CrystEngComm*, 2004, **6**, 130-158; M. Nishio, M. H. Y. Umezawa, *The CH/ $\pi$  interaction (Evidence, Nature and consequences)*, Wiley-VCH, 1998; M. H. Y. Umezawa, S. Tsuboyama, K. Honda, J. Uzawa and M. Nishio, *Bull. Chem. Soc. Jpn.*, 1998, **71**, 1207-1213; C. Janiak, S. Temizdemir, S. Dechert, W. Deck, F. Girgsdies, J. Heinze, M. J. Kolm, T. G. Scharmann and O. M. Zipffel, *Eur. J. Inorg. Chem.*, 2000, 1229-1241.

16  $\pi$ -Interactions between pyridyl-type ligands for comparison: V. Lozan, P.-G. Lassahn, C. Zhang, B. Wu, C. Janiak, G. Rheinwald and H. Lang, *Z. Naturforsch. B*, 2003, **58**, 1152-1164; C. Zhang and C. Janiak, *Z. Anorg. Allg. Chem.*, 2001, **627**, 1972-1975; C. Zhang and C. Janiak, *J. Chem. Crystallogr.*, 2001, **31**, 29-35; H.-P. Wu, C. Janiak, G. Rheinwald and H. Lang, *J. Chem. Soc., Dalton Trans.*, 1999, 183-190; C. Janiak, L. Uehlin, H.-P. Wu, P. Klüfers, H. Piotrowski and T. G. Scharmann, *J. Chem. Soc., Dalton Trans.*, 1999, 3121-3131; H.-P. Wu, C. Janiak, L. Uehlin, P. Klüfers and P. Mayer, *Chem. Commun.*, 1998, 2637-2638.

17 X.-J. Yang, F. Drepper, B. Wu, W.-H. Sun, W. Haehnel and C. Janiak, *Dalton Trans.*, 2005, 256-267 and ESI therein;

18 N. N. L. Madhavi, A. K. Katz, H. L. Carrell, A. Nangia and G. R. Desiraju, *Chem. Commun.*, 1997, 1953-1954; H.-C. Weiss, D. Bläser, R. Boese, B. M. Doughan and M. M. Haley, *Chem. Commun.*, 1997, 1703-1704; T. Steiner, M. Tamm, B. Lutz and J. van der Maas, *Chem. Commun.*, 1996, 1127-1128; P. L. Anelli, P. R. Ashton, R. Ballardini, V. Balzani, M. Delgado, M. T. Gandolfi, T. T. Goodnow, A. E. Kaifer, D. Philp, M. Pietraszkiewicz, L. Prodi, M. V. Reddington, A. M. Z. Slawin, N. Spencer, J. F. Stoddart, C. Vicent and D. J. Williams, *J. Am. Chem. Soc.*, 1992, **114**, 193-218.



**Scheme S2** Graphical presentation of the parameters used for the description of CH- $\pi$  interactions.

Packing Analysis for possible **CH- $\pi$  interactions** (see Scheme S1 for explanation):

=====

Analysis of X-H...Cg( $\pi$ -Ring) Interactions(H..Cg < 3.0 Ang. - Gamma < 30.0 Deg)

=====

- Cg(J) = Center of gravity of ring J(Plane number above)
- H-Perp = Perpendicular distance of H to ring plane J
- Gamma = Angle between Cg-H vector and ring J normal
- X-H..Cg = X-H-Cg angle(degrees)
- X..Cg = Distance of X to Cg(Angstrom)
- X-H,  $\pi$  = Angle of the X-H bond with the  $\pi$ -plane(i.e.' Perpendicular = 90 degrees, Parallel = 0 degrees)

**Table S9** Analysis of X-H...Cg( $\pi$ -Ring) Interactions in 5.

X--H(I)	Cg(J)	[ARU(J)]	H..Cg	H-Perp	Gamma	C-H..Cg	C..Cg	X-H, $\pi$
C(9)-H(9)	->Cg(8)	[4547.01]	2.95	2.89	12.05	140	3.734(7)	53
C(11)-H(11)	->Cg(8)	[4556.01]	2.95	-2.91	9.17	138	3.709(8)	54
		Min. or max.	2.950	-2.907	9.2	140	3.709	54.0

[4547] = 1/2-X,-1/2+Y,2-Z

[4556] = 1/2-X,1/2+Y,1-Z

Ring8: C1-C2-C3-C4-C5-C6

**Table S10** Analysis of X-H...Cg( $\pi$ -Ring) Interactions in 7.

X--H(I)	Cg(J)	[ARU(J)]	H..Cg	H-Perp	Gamma	C-H..Cg	C..Cg	X-H, $\pi$
C(2)-H(2)	->Cg(1)	[1555.01]	2.69	-2.65	9.1	101	3.023(17)	3
C(6)-H(6)	->Cg(15)	[4565.01]	3.00	-2.96	9.13	138	3.758(16)	57
C(12)-H(12)	->Cg(16)	[4565.01]	2.91	-2.83	13.87	142	3.707(18)	59
		Min. or max.	2.690	-2.959	9.1	142.0	3.023	59.0

[1555] = X,Y,Z

[4565] = 1/2+X,1-Y,Z

Ring1: C1-C2-C3-C4-C5-C6

Ring15: C14-C15-C16-C17-C18-C19

Ring16: C20-C21-C22-C23-C24-C25

**Table S11** Analysis of X-H...Cg( $\pi$ -Ring) Interactions in **8**.

X--H(I)	Cg(J)	[ARU(J)]	H..Cg	H-Perp	Gamma	C-H..Cg	C..Cg	X-H, $\pi$
C(6)-H(6)	->Cg(1)	[4564.01]	2.88	2.73	18.77	123	3.49(2)	51
C(9)-H(9)	->Cg(2)	[4555.01]	2.86	-2.80	12.04	133	3.57(3)	51
C(12)-H(12)	->Cg(2)	[4564.01]	2.87	2.84	8.02	139	3.64(2)	54
	Min. or max.		2.860	-2.801	8.0	139	3.490	54.0

[4564] = X,1-Y,-1/2+Z

[4555] = X,-Y,1/2+Z

Ring1: C1-C2-C3-C4-C5-C6

Ring2: C7-C8-C9-C10-C11-C12

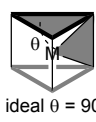
**Table S12** Angles ( $^{\circ}$ ) for comparison of octahedral and trigonal prismatic geometry in **7**. Angles between planes of atoms are denoted with plane through atoms / plane through atoms.

Cd-polyhedra with atom numbers (symmetry labels not given)

octahedron	trigonal prism	geometric relation	angle	averaged	
$\theta_{\text{ideal}}: 54.7$	$\theta_{\text{ideal}}: 90$	O1 O7 <sup>vii</sup> O9 <sup>xiv</sup> / O4 <sup>iii</sup> Cd1 O9 <sup>xiv</sup>	63.2		
		O1 O7 <sup>vii</sup> O9 <sup>xiv</sup> / O1 Cd1 O2	86.1	<u>71.9</u>	
		O1 O7 <sup>vii</sup> O9 <sup>xiv</sup> / O3 <sup>x</sup> Cd1 O7 <sup>vii</sup>	66.3		
		O6 O8 <sup>vi</sup> O10 <sup>xii</sup> / O9 <sup>xii</sup> Cd2 O10 <sup>xii</sup>	68.2		
		O6 O8 <sup>vi</sup> O10 <sup>xii</sup> / O2 Cd2 O6	75.4	<u>77.3</u>	
		O6 O8 <sup>vi</sup> O10 <sup>xii</sup> / O1 <sup>x</sup> Cd2 O8 <sup>vi</sup>	88.4		
		O3 O5 <sup>i</sup> O6 / O5 Cd3 O10 <sup>i</sup>	69.1		
		O3 O5 <sup>i</sup> O6 / O3 Cd3 O7 <sup>vi</sup>	79.0	<u>79.1</u>	
		O3 O5 <sup>i</sup> O9 / O6 Cd3 O8	89.2		
		O3 <sup>x</sup> Cd1 O9 <sup>xiv</sup>	158.4(3)		
$\rho_{\text{ideal}}: 180$	$\rho_{\text{ideal}}: 135.4$	O4 <sup>iii</sup> Cd1 O1	158.0(3)	<u>151.9</u>	
		O7 <sup>vii</sup> Cd1 O2	139.4(3)		
		O2 Cd2 O8 <sup>vi</sup>	157.5(3)		
		O1 <sup>xi</sup> Cd2 O10 <sup>xii</sup>	126.4(3)	<u>141.0</u>	
		O6 Cd2 O9 <sup>xii</sup>	139.0(3)		
		O3 Cd3 O10 <sup>i</sup>	154.6(3)		
		O5 <sup>i</sup> Cd3 O8	144.2(3)	<u>144.4</u>	
		O7 <sup>vi</sup> Cd3 O6	134.4(3)		
		O1 O2 Cd1 / O4 <sup>iii</sup> O9 <sup>xiv</sup> Cd1	115.8		
		O1 O2 Cd1 / O3 <sup>x</sup> O7 <sup>vii</sup> Cd1	107.2	<u>110.5</u>	
$\omega_{\text{ideal}}: 180$	$\omega_{\text{ideal}}: 120$	O4 <sup>iii</sup> O9 <sup>xiv</sup> Cd1 / O3 <sup>x</sup> O7 <sup>vii</sup> Cd1	108.6		



ideal  $\theta = 54.7^{\circ}$



ideal  $\theta = 90^{\circ}$

$\theta$  = angle between the mean plane of the two  $O_3$  triangles and the chelate planes defined by the metal and each pair of near eclipsed O vertices

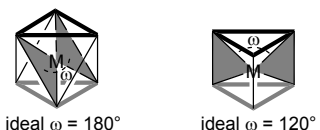


ideal  $\rho = 180^{\circ}$



ideal  $\rho = 135.4^{\circ}$

$\rho$  = angle between the metal and *trans* O-donor sites.



O2 O6 Cd2 / O1 <sup>x</sup> O8 <sup>vi</sup> Cd2	139.0		
O2 O6 Cd2 / O9 <sup>xii</sup> O10 <sup>xii</sup> Cd2	119.9		<u>116.5</u>
O1 <sup>x</sup> O8 <sup>vi</sup> Cd2 / O9 <sup>xii</sup> O10 <sup>xii</sup> Cd2	90.8		
O6 O8 Cd3 / O7 <sup>vi</sup> O3 Cd3	114.6		
O3 O7 <sup>vi</sup> Cd3 / O5 <sup>i</sup> O10 <sup>i</sup> Cd3	115.7		<u>116.7</u>
O6 O8 Cd3 / O5 <sup>i</sup> O10 <sup>i</sup> Cd3	119.9		

$\omega$  = angle between the triangular faces defined by the metal and near eclipsed O atoms.

Symmetry transformations: i = 1/2-x, y, 1/2+z; ii = 1/2-x, y, -1/2+z; iii = -x, 2-y, 1/2+z; iv = v = -1/2+x, 1-y, z; vi = 1/2+x, 1-y, +z; vii = x, -1+y, z; ix = 1/2+x, 2-y, z; x = -1/2+x, 2-y, z; xii = -x, 1-y, 1/2+z; xiii = 1/2-x, -1+y, -1/2+z; xiv = 1/2-x, 1+y, 1/2+z.

**Table S13** Dihedral angles between aryl rings in the biphenyl system and between –COO(H) group and ary rings in **5-8**.

	<b>5</b>	<b>6</b>	<b>7</b>	<b>8</b>
Biphenyl, dihedral	0.1(6)	1.5(1)	0.5(2)	2.0(2)
-COO(H) group to benzyl, dihedral	16.3(9)	2(2)	2.0(2)	5.0(4)

### Circular Dichroism spectra of **5**

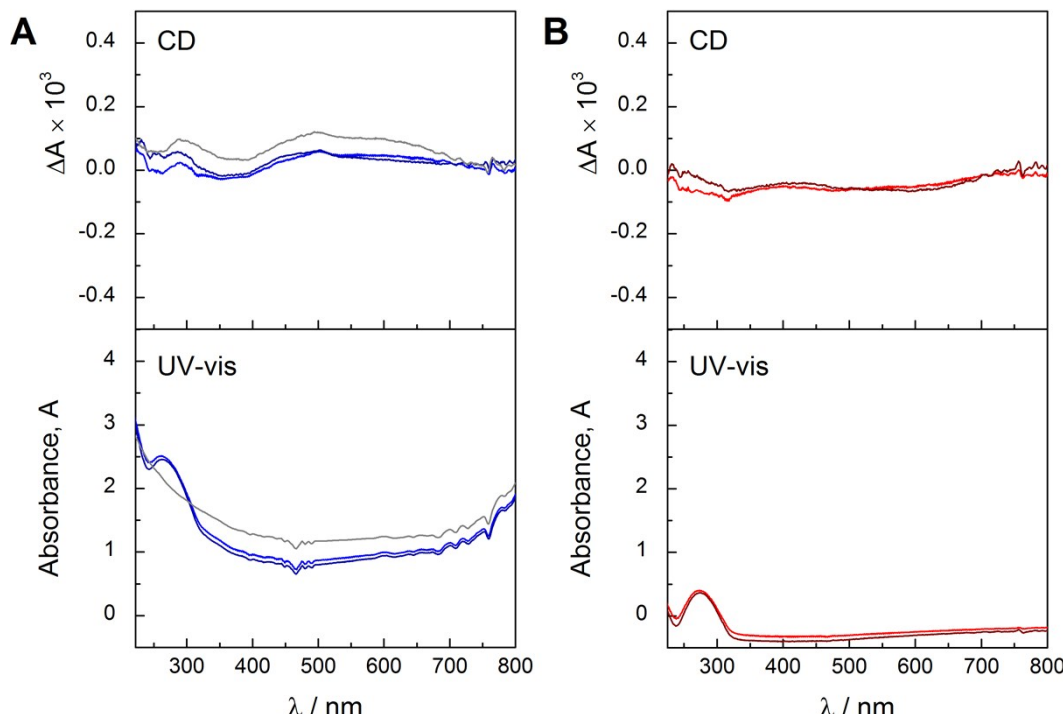


**Figure S33** Solid state UV-visible and CD spectroscopy of the zinc compound  $[\text{Zn}_5(\mu_3\text{-OH})_4(\mu_4\text{-O}_3\text{P-(C}_6\text{H}_4)_2\text{-CO}_2\text{-}\mu_2)_2]$  (**5**) performed with KBr pellets (0.05 wt% of **5**). The blue curves in A are the

results from two independent measurements. The gray curve represents the background recorded for a pellet of pure KBr. The red spectra in B are the background-corrected spectra from A and do not contain any significant spectral features that would indicate enantiomeric excess of either one of the two possible enantiomers of **5**.